NASA CR-937

DYNAMIC STABILITY OF SPACE VEHICLES

Volume III - Torsional Vibration Modes

By R. Gieseke, R. Schuett, and D. Lukens

Issued by Originator as Report No. GD/C-DDF65-003

Prepared under Contract No. NAS 8-11486 by
GENERAL DYNAMICS CORPORATION
San Diego, Calif.

for George C. Marshall Space Flight Center

NATIONAL AERONAUTICS AND SPACE ADMINISTRATION

For sale by the Clearinghouse for Federal Scientific and Technical Information
Springfield, Virginia 22151 – CFSTI price $3.00

FOREWORD

This report is one of a series in the field of structural dynamics prepared under contract NAS 8-11486. The series of reports is intended to illustrate methods used to determine parameters required for the design and analysis of flight control systems of space vehicles. Below is a complete list of the reports of the series.

Volume I	Lateral Vibration Modes
Volume II	Determination of Longitudinal Vibration Modes
Volume III	Torsional Vibration Modes
Volume IV	Full Scale Testing for Flight Control Parameters
Volume V	Impedence Testing for Flight Control Parameters
Volume VI	Full Scale Dynamic Testing for Mode Determination
Volume VII	The Dynamics of Liquids in Fixed and Moving Containers
Volume VIII	Atmospheric Disturbances that Affect Flight Control Analysis
Volume IX	The Effect of Liftoff Dynamics on Launch Vehicle Stability and Control
Volume X	Exit Stability
Volume XI	Entry Disturbance and Control
Volume XII	Re-entry Vehicle Landing Ability and Control
Volume XIII	Aerodynamic Model Tests for Control Parameters Determination
Volume XIV	Testing for Booster Propellant Sloshing Parameters
Volume XV	Shell Dynamics with Special Applications to Control Problems

The work was conducted under the direction of Clyde D. Baker and George F. McDonough, Aero Astro Dynamics Laboratory, George C. Marshall Space Flight Center. The General Dynamics Convair Program was conducted under the direction of David R. Lukens.

TABLE OF CONTENTS

1.	INTRODUCTION		1
2.	STATE-OF-THE-ART		5
3.	MODEL REQUIREMENTS AND RECOMMENDED PROCEDURES		7
	3.1	Cylindrical Liquid Propellant Vehicle	9
		3.1.1 Selection of Inertia	10
		3.1.2 Liquid Propellant Effects	11
		3.1.3 Engine Representation	13
		3.1.4 Branch Shafts	13
		3.1.5 Local Structure Effects	13
		3.1.6 Temperature	14
		3.1.7 Axial Load	14
		3.1.8 Lateral-Torsional-Longitudinal Coupling	15
		3.1.9 Damping Effects	15
	3.2	Adding Components Using Mode Synthesis	16
	3.3	Correcting Model Based on Test Results	17
	3.4	Solid Boosters	17
	3.5	Clustered Boosters	18
4.	METHODS FOR SOLUTION		23
	4.1	Formation of the Coupled Equations	23
		4.1.1 Stiffness Matrix	23
		4.1.2 Flexibility Matrix	28
		4.1.3 Transformed Mass Matrix	31
	4.2	Solutions for Characteristics	33
		4.2.1 Matrix Iteration (Stodola and Vianello Method)	33
		4.2.2 Holzer (Myklestad)	33
		4.2.3 Energy Methods (Rayleigh-Ritz)	33
		4.2.4 Modal Quantities	34

4.3 Mode Synthesis Analysis 34

4.4 Example of Coupled Bending-Torsion Analysis 34

4.4.1 Stiffness Matrix Solution 35

4.4.2 Mode Synthesis Solution 37

4.4.3 Comparison of Solutions 40

5 REFERENCES 55

LIST OF ILLUSTRATIONS

1.	Simple Torsional System	7
2.	Uniform Cantilevered Shaft – Natural Frequencies Continuous Solution and Lumped Parameter Solution	12
3.	Engine Representation	13
4.	Example of Branched System	14
5.	Titan IIIC	20
6.	Saturn I Block II Connection Details	22
7.	Complex Torsional System	23
8.	Cantilevered Linearily Varying Stiffness Beam	24
9.	Coefficient of Equivalent Stiffness – Linearly Varying Stiffness Shaft	26
10.	Cantilevered Torsional System	29
11.	Sample Bending Torsion System	35
12.	Analytical Model of Sample System	36
13.	Separation of Model Into Components	37

LIST OF TABLES

1.	Frequency Coefficients for Lumped Cantilevered System	11
2.	Non-zero Elements of the Upper Triangle of the Sample Coupled System Unrestrained Stiffness Matrix	42

NOMENCLATURE

C	Flexibility matrix
D	Dynamic matrix
E	Young's modulus; spring rate
F	Forcing function matrix
f	Function, e.g., f(X); frequency
G	Shear modulus
I	Area Moment of Inertia
I_i	Mass moment of inertia
i	Coordinate index
J	Polar area moment of inertia
j	Coordinate index
K	Stiffness matrix
K_c	Stiffness matrix of connecting elements - mode synthesis
k	Element stiffness or spring rate
L	Shaft length; subscript for lateral
ℓ	Beam length
M	Mass inertia matrix; total moment
m	Incremental moment; meter
$\mathfrak{m}$	Generalized mass
n	Mode index
Q	Generalized force
q	Generalized coordinate
R	Incremental load/total load transform matrix
T	Relative displacement/absolute displacement transform matrix
t	Time
U	Deflection amplitude
W	Work
X	Lateral displacement coordinate

x, y, z	Cartesian coordinates
β	Rigid body angular displacement; beam bending angular displacement coordinate
Δ	Connecting element deformation - mode synthesis
η	Modal weighting factor - mode synthesis
Θ	Rigid body torsional rotation
θ	Torsional displacement coordinate
υ_o	Rotation of fixity point upon release
ξ	Damping factor
ρ	Mass density
Φ	Matrix of mode shapes
ϕ	Eigeinvector
ω	Natural circular frequency
kg	Kilogram
n - m	Newton - Meter
$(\dot{})$	A dot over a symbol indicates first time derivative
$(\ddot{})$	Two dots over a symbol indicates second time derivative
[ ]	Square matrix
[ ]	Diagonal matrix
{ }	Column matrix

1/INTRODUCTION

This monograph discusses the torsional model development and modal calculations for the cylindrical space vehicle system and also systems employing clustered tanks. Relative importance of physical characteristics will be discussed as well as methods used by the industry for the solution of modal parameters. Primary attention is focused on parameters important in control and stability analyses for which the system frequency is generally below twenty cycles per second and quite often below ten cycles per second. Application for loads analysis follows the same principals outlined herein but may require more detailed representation in areas where loads or deflections can be critical. The models described will be concerned with gross vehicle torsional motions and will not include the shell tangential deflection modes which do not contribute to gross vehicle control and stability. Related monographs describe lateral, longitudinal, and sloshing models. Stability and loads analytical methods using these models and modal parameters are also subjects of other monographs.

The general approach for dynamic solutions involving large systems is to develop a mathematical model describing the system's mass and structure, calculate its normal modes of vibration, and then, using normal mode theory, apply the external forces and couple in the control system to obtain total response. The dynamic analysis is then only as accurate as provided by the mathematical model representing the space vehicle system; therefore, development of these models is of major importance in dynamic analysis. Also, since these models are idealizations and approximations of the real system, the experience of an analyst in deciding which elements are dominant contributes greatly to the successful representation of the system.

Space launch vehicles are primarily cylindrical structures comprised of propellant tanks and interstage adapters. The rocket engines are attached to the propellant tanks in a symmetrical pattern and the major payload structure and weight distribution is usually symmetric. This arrangement allows little, if any, coupling between the lower longitudinal, lateral, and torsional modes. For liquid vehicles, the effective mass considered in torsion is primarily structure and components, neglecting liquid because of its limited shear resistance. As a result, the frequencies of the torsional modes are usually well separated from the frequencies of the primary bending and longitudinal modes which consider the total vehicle mass. This frequency separation, plus the vertical axis symmetry in the bending and longitudinal models, and the symmetry of the structure, are reasons for the absence of significant coupling between the modes. Also, since most vehicles are axis-symmetric with respect to applied forces, such as aerodynamics and engine thrust, these are not significant causes of torsion excitation.

Later in flight, as propellants are depleted, the modes can become coupled because of less frequency separation and the loss of axial symmetric weight distribution.

The torsional frequencies, usually greater than twenty cps, still remain outside of control system interest. The only known torsional problems in cylindrical vehicles are shocks and short duration periodic transients caused by engine transients or aerodynamic shock.

A good example is the transient at booster engine shutdown of the Atlas vehicle. Engine pressure oscillations (about 60 to 70 cps) for a duration of about 10 cycles results in longitudinal input to the vehicle. This excites longitudinal, lateral, torsional, and shell modes with frequencies in the same range. Since these are higher modes and are not described well analytically (or experimentally), and also because the coupling mechanism is difficult to define, this condition has not been satisfactorily analyzed. It is known that the payload characteristics are contributors to the torsional response since its stiffness and inertia distribution can cause a torsional mode frequency to be in the 60 to 70 cps region.

Large diameter boosters, such as the Saturn V, will have torsional modes at lower frequencies, below 10 cps, but will remain well separated from the lower lateral modes. Coupling with longitudinal modes would only be a second order effect. With bending and torsional frequencies reduced, but separated, it should be possible to design a control system for stability of the bending and sloshing modes and keep the torsion modes outside of the control system frequency response range. Torsional loads again will only be important if excitation in roll (peculiar to the system) exists.

The advent of clustered boosters introduces a new generation of torsional problems. The torsional mode frequencies will not be separated from the lateral and longitudinal mode frequencies and the configurations will usually be subjected to pronounced bending-torsion coupling. Torsional excitation will probably be induced through lateral excitation and control system behavior and will require extensive torsion, torsion-bending, and control system analyses.

The analysis of the torsional dynamics of a space vehicle requires the development of a mathematical model to represent the characteristics of the actual vehicle undergoing angular deformations about its longitudinal axis. In its simplest form, the model is a set of mass inertias connected in series by rotational springs. By successive refinements, the model can be brought to represent all significant motions of the vehicle. Such refinements can include branched systems to represent multiple load paths, or special treatment for locally significant components.

The analyses of boosters with clustered tanks becomes more complicated for several reasons: 1) the attaching structure is generally complex and, hence, is more difficult to represent; 2) the structure requires more coordinates for adequate representation, and 3) the possibility for coupled response forms (such as bending-torsion) is increased. The analysis technique for a clustered booster is basically the same as for the cylindrical tank, however, the necessity for larger numbers of coordinates

can easily lead to excessive demands on computer storage capacity, which may precipitate a need for a compromise between the accuracy of results and the efficiency and capability of present computer facilities.

2/STATE-OF-THE-ART

The earliest applications of torsional vibration analysis will be found in the area of rotating shaft machinery. The classical continuous solution has been used extensively, as well as approximate numerical solutions. This subject has been studied so extensively that handbooks (such as Reference 1) have been prepared to assist the mechanical designer by providing numerous formulae for the calculation of moments of inertia for flywheels, journals, couplings, ship propellers, gears and crankshafts; stiffness formulae for shafts of uniform and tapered diameter, solid or bored shafts, slotted, splined, rectangular, and asymmetrical shafts. Several different tabular and graphical methods of frequency determination have been developed, but most are variations of the approximate analyses technique developed by Holzer.

Holzer's method (Reference 2) presents a technique for analyzing nonuniform shafts that can be represented by inertias connected by clock springs. With the advent of electronic computers, very accurate torsional mode shapes and frequencies can be obtained for systems which can be represented by interconnected springs and inertias. Figure 2, Section 3, gives a comparison of uniform cantilevered shaft frequencies obtained by the classic solution and the approximate solution using lumped inertias and springs.

In aircraft design, the investigation of wing dynamics frequently requires the analysis of a system coupled in torsion and bending. The wing is represented by a beam of variable stiffness with masses lumped at points eccentric to the beam elastic center line. A full vibration analysis yields coupled mode shapes. The relative contributions of bending and torsion to these mode shapes may be seen by noting that the elastic center line deflection is unaffected by torsion and that torsion alone creates the differences in deflections between the center line and the offset masses.

Torsion of cylindrical space launch vehicles has been treated by considering the system as a series of lumped inertias connected by rotation springs. The spring represents the torsional stiffness of the walls between inertia stations. The inertia, for liquid vehicles, is the polar moment of inertia of the structure and components. For solid motors, the inertia includes all of the propellant. The engine compartments and payloads are described by equivalent springs and inertias, often obtained from test data. The approximate methods of Holzer, matrix iteration, etc., are generally used to obtain the modal quantities.

Vibration tests to determine torsional modes of this class of vehicle have not been conducted, primarily because these modes are of no interest since they are uncoupled from lateral and longitudinal motion, and because no major defined excitation exists during flights. In the case of the Atlas transients at engine shutdown, a vibration test was not justified because it would only describe modes and frequencies, and not the coupling mechanisms causing the torsional response.

The torsional vibration of clustered vehicles has been considered by combining bending and torsion in the mathematical model.

A superimposed normal mode torsional analysis, similar to the bending analysis in Reference 3, has been used in analyzing torsional vibrations of Saturn vehicles for the past three years. No description of the method has been published, however. Milner (Reference 4) proves the uncoupling of torsional and bending modes for a bisymmetric vehicle. In this analysis, the torsional modes of a center beam which consists of the upper stages and the center tank of the booster are coupled with the bending modes of the outer tanks. Torsional modes of the outer tanks are neglected since the energy content of these modes is small and the frequencies are above the region of interest.

Agreement of predicted modes with dynamic test data is generally good. However, some unnecessary limitations exist in the present model which limit the usefulness. For example, only one bending mode of the outer tanks is included in the present model, limiting the results to frequencies below the second mode of the outer tanks. A major limitation on checking accuracy of the method has been the problem of estimating accuracy of the input torsional data.

The coupling of outer tank bending and center tank torsion has also been considered in the analysis of Titan IIIC (Reference 5).

3/MODEL REQUIREMENTS AND RECOMMENDED PROCEDURES

The solution of dynamics problems requires first, the formation of the governing equations, second, their solution to yield dynamic characteristics (eigenvalues, eigenvectors), and, finally, the calculation of system response to external load through the use of the modal information.

The governing equations are developed through consideration of equilibrium requirements or energy relationships. To illustrate the basic technique of developing these equations, the simple torsional system of Figure 1 will be considered. The displacement of each mass inertia is defined by θ_1, θ_2, θ_3.

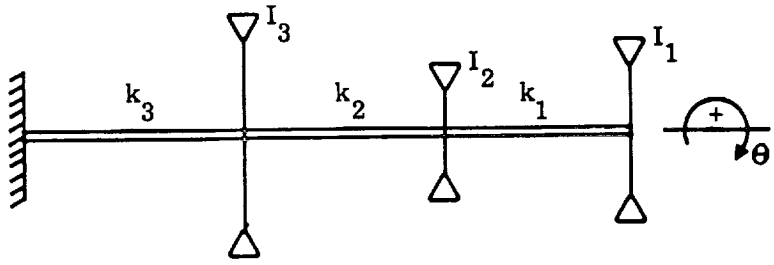

Figure 1. Simple Torsional System

In a deformed position, all the internal forces of the system are readily determined. The internal moment developed in the spring k_1 acts on I_1 as $-k_1 (\theta_1 - \theta_2)$, and on I_2 as $k_1 (\theta_1 - \theta_2)$. Similarly, the internal moment developed in spring k_2 is $-k_2 (\theta_2 - \theta_3)$ on I_2 and $k_2 (\theta_2 - \theta_3)$ on I_3. The moment from spring k_3 will be $-k_3 (\theta_3)$ on I_3. Applying Newton's second law of motion ($\Sigma F = ma$ or $\Sigma M = I\ddot{\theta}$) to each mass inertia results in

$$I_1 \ddot{\theta}_1 = - k_1 (\theta_1 - \theta_2) \tag{1}$$

$$I_2 \ddot{\theta}_2 = k_1 (\theta_1 - \theta_2) - k_2 (\theta_2 - \theta_3) \tag{2}$$

$$I_3 \ddot{\theta}_3 = k_2 (\theta_2 - \theta_3) - k_3 \theta_3 \tag{3}$$

which are the desired governing equations.

The same equations are obtained by generating, kinetic and potential energy expressions for the system and introducing them into the LaGrange equation

$$\frac{\partial}{\partial t} \left[\frac{\partial (KE)}{\partial \dot{q}}\right] + \frac{\partial (PE)}{\partial q} + \frac{\partial W}{\partial q} = 0 \tag{4}$$

For the system under investigation, the kinetic energy is $\sum_{i=1}^{3} \frac{1}{2} I_i \dot{\theta}_i^2$ and the potential energy is $\sum_{i=1}^{3} \frac{1}{2} k_i (\Delta\theta)_i^2$ where $\Delta\theta_1 = \theta_1 - \theta_2$, $\Delta\theta_2 = \theta_2 - \theta_3$, and $\Delta\theta_3 = \theta_3$.

Substitution in the Lagrange equation yields

$$I_1 \ddot{\theta}_1 + k_1 (\theta_1 - \theta_2) = 0 \tag{5}$$

$$I_2 \ddot{\theta}_2 - k_1 (\theta_1 - \theta_2) + k_2 (\theta_2 - \theta_3) = 0 \tag{6}$$

$$I_3 \ddot{\theta}_3 - k_2 (\theta_2 - \theta_3) + k_3 \theta_3 = 0 \tag{7}$$

It should be noted that the system is considered undamped and free from external forces. The general form of the governing equations is such that they may be expressed in matrix notation as

$$[M] \{\ddot{\theta}\} + [k] \{\theta\} = \{F\} \tag{8}$$

where for modal calculations, $F = 0$.

If simple harmonic motion is assumed, this becomes

$$-\omega^2 [M] \{\theta\} + [k] \{\theta\} = 0 \tag{9}$$

or

$$\theta = \omega^2 [k]^{-1} [M] \{\theta\} \tag{10}$$

Either of these equations is in a form suitable for the solution for the elastic orthogonal modes (eigenvectors, ϕ) and their natural frequencies (ω). Several selected techniques of solution are described in Section 4.2.

The dynamic response of the system to applied external loads may be described through the use of normal mode theory. The time dependent motion of the system may be described in terms of the natural modes of vibration (ϕ) as

$$\theta_i = \sum_n \phi_{in} q_n \quad \text{or} \quad \{\theta\} = [\phi] \{q\} \tag{11}$$

q_n is the time dependent amplitude of the mode n. This can be substituted into equation 8 to yield

$$[M][\phi]\{\ddot{q}\} + [k][\phi]\{q\} = \{F\} \tag{12}$$

from whence it follows that

$$[\phi]'[M][\phi]\{\ddot{q}\} + [\phi]'[k][\phi]\{q\} = [\phi]'\{F\} \tag{13}$$

By reasons of orthogonality, the matrix formed by $[\phi]'[M][\phi]$ is a diagonal matrix of generalized masses, and is expressed as $[\mathfrak{m}]$. Further, the matrix formed by $[\phi]'[k][\phi]$ is the diagonal generalized stiffness matrix. If the generalized stiffness is divided by the generalized mass, the result is the square of the natural circular frequency, ω^2. Consequently, dividing Equation 13 through by $[\mathfrak{m}]$ yields

$$\{\ddot{q}\} + [\omega^2]\{q\} = [\mathfrak{m}]^{-1}[\phi]'\{F\} \tag{14}$$

These equations are uncoupled, permitting each mode to be treated individually.

$$\ddot{q}_n + \omega_n^2 q_n = \frac{Q_n(t)}{\mathfrak{m}_n} \tag{15}$$

where $Q_n(t) = \sum_i \phi_{in} F_i$ and $\mathfrak{m}_n = \sum_i I_i \phi_{in}^2$

Equation 15 may be solved to yield time dependent values of q_n which may then be used in Equation 11 to obtain total system response.

The above description displays the basic procedure in the solution of dynamics problems. The mathematical model used is the key to the entire study, and its proper development is vital to the analysis. Therefore, it is justified to dwell at length on the manner in which the model is formed and the factors which influence its development, as well as some techniques of solution.

3.1 CYLINDRICAL LIQUID PROPELLANT VEHICLE

Frequently, the torsional characteristics of the cylindrical liquid propellant vehicle can be adequately defined by using a simple shaft model. In the vast majority of cases it will be either necessary or more practical to construct the model using a lumped parameter idealization. In its fundamental form, the model attempts to duplicate the effects of major aspects of the vehicle (primary structure, major mass concentrations, etc.). The discrete model is formed by concentrating the distributed inertias into distinct inertias at selected points along the shaft. The concentrated

inertia which is to represent a certain area under an inertia distribution curve should ideally be located at the centroid of that area.

Once the concentrated inertias have been located, thus defining the shaft segments, the torsional elasticity between concentrated inertias is developed from the dimensional and material properties of the shaft segment and is generally represented by a torsional spring with a rate, k, which duplicates the elastic behavior of the shaft it replaces. The development of torsional spring rates is examined in Section 4.1.

3.1.1 SELECTION OF INERTIA. The polar moment of inertia to be considered is composed of vehicle structure and components. Components are often placed around the periphery of adapter structure and will be a significant portion of the total inertia. These components can be considered as rigidly attached if their mount frequencies are greater than the frequencies of the torsional modes to be considered. If the mount frequencies are lower, then the component must be attached elastically, possibly through lateral and torsional springs on a rigid arm an appropriate distance from the tank centerline.

The number of concentrated inertias given to the model determine the number of degrees of freedom of the system, and thus, the number of simultaneous governing equations. As the number of degrees of freedom increase, the model approaches the continuous system, but the solution becomes more difficult. At some point a trade-off must be made between accuracy and practicality.

To illustrate the relationship between accuracy and degrees of freedom of the discrete model, consider a uniform cantilevered shaft. Its natural frequencies are readily obtained via the classical solution as a continuous system and are

$$\omega_n = (2n-1)\frac{\pi}{2}\sqrt{\frac{G}{\rho L^2}} \tag{16}$$

where ω_n is the n^{th} natural circular frequency, G is the shear modulus of the material, ρ is mass density, and L is the length of the shaft.

Let this shaft now be represented by a system of mass inertias connected in series by rotational springs, and connected to a rigid base at one end. For a given system of i inertias, each inertia will have the value of $\frac{J\rho L}{i}$. Each spring will have a spring rate of $\frac{JGi}{L}$. J is the polar moment of inertia of the shaft cross section. The frequencies of lumped uniform systems are given by, from Reference 6,

$$\omega_n = \sqrt{\frac{Z_n\, i^2 G}{\rho L^2}} = C_{in}\sqrt{\frac{G}{\rho L^2}} \tag{17}$$

where $Z_n = 2 \left(1 - \cos \frac{2n-1}{2i+1} \pi \right)$

Values for $C_{in} = i \sqrt{Z_n}$ are given in Table 1. Figure 2 gives a comparison of the frequency coefficients obtained from each discrete system and the coefficients of the continuous system. The data indicate reasonable accuracy is obtained with ten inertias for the first mode. The accuracy of higher modes degenerates rapidly with increasing order.

Table 1. Frequency Coefficients for Lumped Cantilevered System

n \ i	1	2	5	10	20	30	50
1	1.0000	1.24	1.43	1.49	1.53	1.55	1.55
2		3.24	4.16	4.45	4.59	4.63	4.66
5			9.60	12.46	13.52	13.80	13.98
10				19.80	26.60	28.20	29.20

Accuracy will be harder to obtain if the shaft is nonuniform, as the discrete model will have to represent the variations in inertia and stiffness distribution. Accordingly, it is suggested that a minimum of 10 inertia terms be used for every mode desired. It should also be mentioned that the law of diminishing returns applies to this aspect of modeling; each additional inertia term increases the accuracy of the model, but to a lesser degree than the one preceding it. Consequently, the use of more than 15 inertias for each mode desired will rarely be justified.

For a more complex model (such as one with branched shafts and components) the above general rule is not strictly applicable. For a branched system, the general rule can be applied to the primary beam of the system, and inertias lumped on the secondary branches in about the same distribution. As the model diverges from the single beam concept, more reliance must be placed upon the experience of the analyst.

3.1.2 LIQUID PROPELLANT EFFECTS. In the case of the liquid propellant vehicle vibrating in pure torsion, the propellant is virtually unexcited. Since the only stress condition is that of shear, the liquid can participate only to the extent allowed by its viscosity. It is most probable that the fluids in the vehicle tanks can be considered nonviscous, and therefore contribute nothing to the inertias. It is evident that under these conditions, the quantity of propellant has no effect on the torsional vibration characteristics of the vehicle, hence these characteristics do not vary with time in flight.

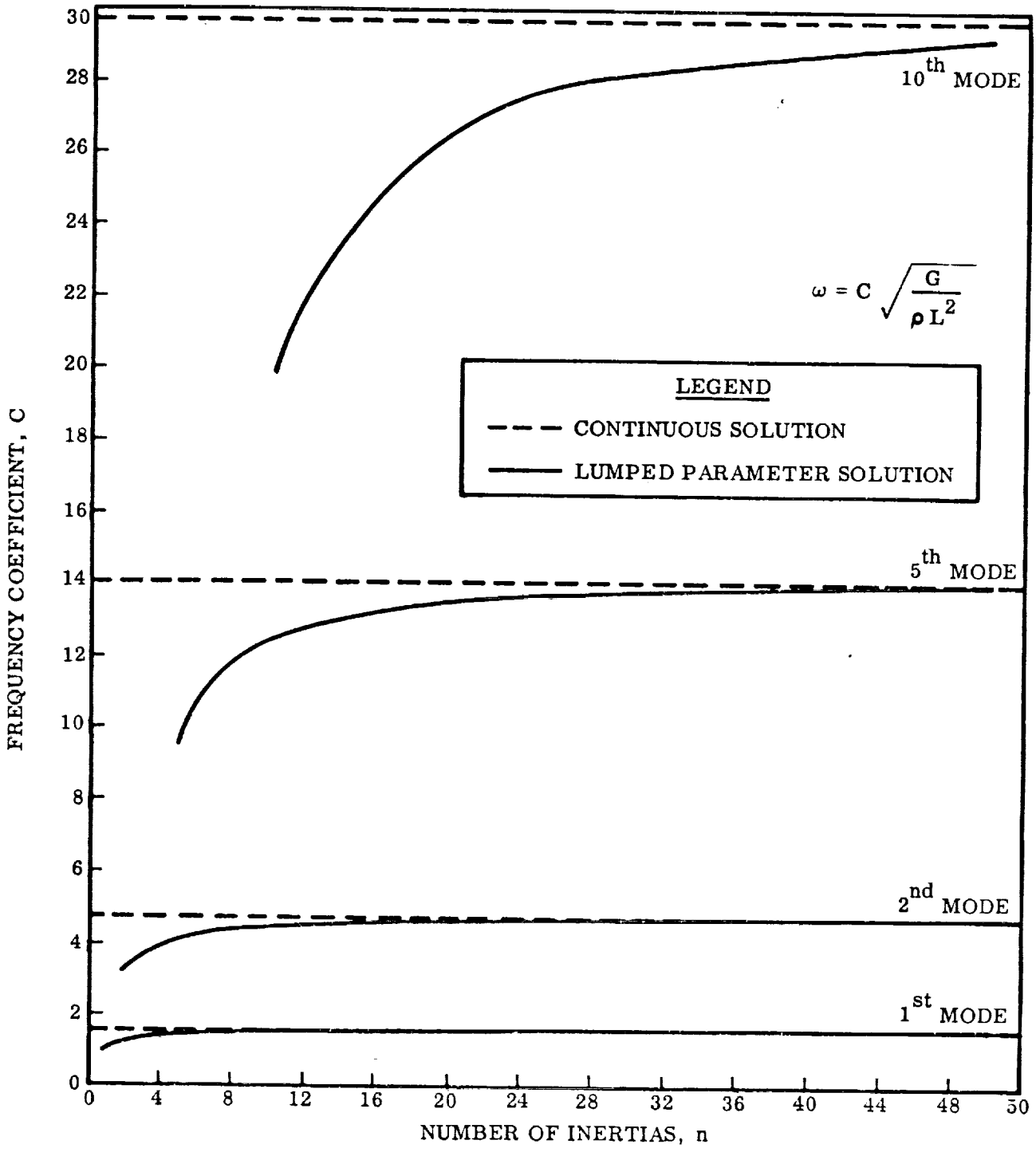

Figure 2. Uniform Cantilevered Shaft – Natural Frequencies Continuous Solution and Lumped Parameter Solution

3.1.3 ENGINE REPRESENTATION. Engines represent a sizeable proportion of vehicle weight (excluding propellants) and are often attached near the tank periphery. Consequently, they are predominant factors in the polar moment of inertia. The engines are incorporated with the torsional modal by attaching a mass and moment of inertia at the appropriate location in the one-dimensional shaft. A rigid bar can be used to locate the engine near the periphery as in Figure 3. This structure is generally complex and test data is often required for proper simulation.

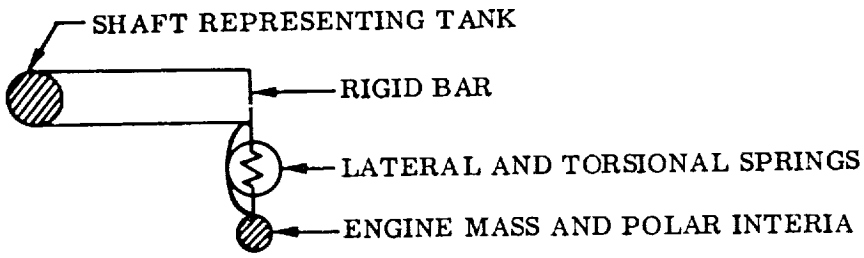

Figure 3. Engine Representation

3.1.4 BRANCH SHAFTS. Frequently the vehicle construction will be such that major portions are cantilevered within another structure or are connected through different load paths, e.g., payloads enveloped by protective fairings, engine compartments of upper stage vehicles suspended in the inter-stage adapter well, or multi-engine vehicles having independent load paths for each engine such as a center engine supported on the tank cone and peripheral engines mounted to the cylindrical structure of the vehicle. Such conditions are illustrated in Figure 4. Realistic representations of these arrangements are required for true definition of gross vehicle response. These multiple paths can be accounted for by appropriate branch shafts from the major center shaft. So long as the analysis is restrained to one dimensional motion, there is no significant added complexity introduced by the branch shafts, since the compatibility relationships at the junction points can be easily satisfied. Note the model in Figure 4. Branch shafts can be attached by 1) secondary shaft elements, as is done for the payload fairing and the upper stage engine structure; or 2) concentrating elasticity in lateral linear and angular springs at ends of rigid bars as is done for the external engines of the booster.

3.1.5 LOCAL STRUCTURE EFFECTS. One of the major difficulties encountered in describing a vehicle is the representation of supporting structure for engines, payloads, and components. It is possible to obtain influence coefficients analytically, but a final check with load deflection tests is advisable if it is probable that this structure can influence the modes of interest.

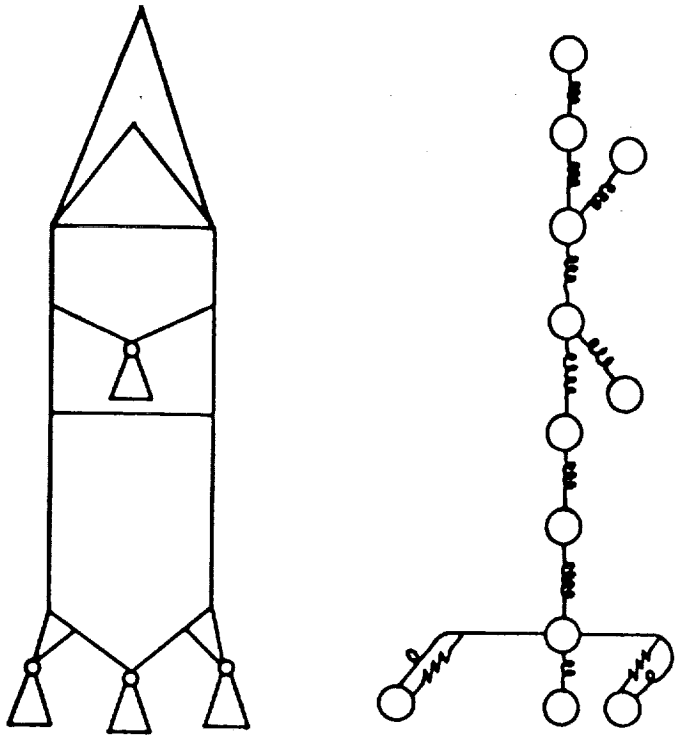

Figure 4. Example of Branched System

3.1.6 TEMPERATURE. Primary structures of space vehicle systems are subjected to change in temperature of hundreds of degrees varying from cryogenic temperatures to the extreme elevated temperatures resulting from aerodynamic heating. This increase in temperature causes a reduction in the material moduli which in turn leads to a small reduction in frequencies and altered mode shapes. Temperature considerations are unimportant until after the period of maximum aerodynamic pressure and then only for certain portions of the vehicle. Since the period of maximum heating occurs after the period of maximum disturbance and only affects parts of the structure, its significance is greatly reduced. The heating of various portions of the vehicle can be predicted within tolerances necessary for modal analyses to establish the resultant variation in modal parameters.

3.1.7 AXIAL LOAD. Axial loads do not alter the expressions of energy or strain associated with torsion except through second and third order terms. The modal analyses are restricted to small displacements and all terms higher than first order are omitted. Therefore, axial load effects should also be omitted.

3.1.8 LATERAL-TORSIONAL-LONGITUDINAL COUPLING. The typical axis symmetric cylindrical space vehicle is analyzed as if lateral, torsional, and longitudinal motion are not coupled. Actually, these vehicles are not completely symmetric and a possible coupling mechanism, however slight, can always be found. The importance of this coupling can vary greatly from vehicle to vehicle. Even if it is known to exist from flight or experimental data, the coupling mechanism is difficult to identify. These coupling problems often occur when the modal frequencies of two modes, say, one lateral and one torsional, are very close together. Then a very small coupling mechanism, such as center of gravity (c.g.) offset from the supposed line of symmetry, can result in coupled motion.

A comparison of the fundamental frequencies of the modes in the three directions should be made to determine the existence of modes of nearly equal frequency. If such a condition exists, it is necessary to examine the condition under which this may cause a significant problem. As an example, if a limit cycle can occur due to sloshing, could this cause excitation of a critical torsional mode at this same frequency or subharmonic? In most instances of coupling of this type, a periodic forcing function is necessary to transmit the energy from one direction to another.

Cylindrical vehicles with unsymmetric upper stages or payloads of large mass can cause coupling in the various directions in the low frequency modes. The model and analysis then becomes complicated and approaches that of the clustered boosters. Representation of this configuration requires detailed description in the unsymmetric stages and proceeding with analysis as described later for clustered boosters. Preliminary work would indicate the degree of sophistication to be used for adequate representation for stability and loads analysis.

3.1.9 DAMPING EFFECTS. Structural dissipative (damping) forces exist in the vibrating structure as a result of material strain hysteresis and coulomb friction in structural joints. The nature of these damping effects is obscure and does not lend itself to analysis other than an approximate empirical treatment, by which the gross effect of these scattered dissipative mechanisms is represented as an equivalent viscous damping, added to each mode as appropriate. The damping is thus assumed to produce no coupling between modes. While this mechanization is not entirely realistic, it is justified by the following observations:

a. The actual damping is very low and is found by test to produce little coupling. Thus, nearly pure normal modes of a system may be excited and the system observed to decay almost harmonically. The indication given is that velocity-dependent coupling is very small.

b. If an attempt is made to show a velocity-dependent coupling, the coefficient would have to be determined experimentally. Since the direct damping coefficient is itself difficult enough to measure, it is clear that the accuracy of a study can not be increased by the introduction of still more suspect data.

The structural damping force is a function of the deflection of the generalized coordinate of the mode but in phase with the velocity of the generalized coordinate of that mode. To treat this damping as a viscous damping requires that the mode oscillate in a quasi-harmonic manner. This damping force may then be expressed as a damping factor, ξ_n, where $2\,\xi_n\,\omega_n\,\dot{q}_n$ is the internal damping force of the n^{th} mode per unit generalized mass.

Equation (15), with damping included, becomes

$$\ddot{q}_n + 2\,\xi_n\,\omega_n\,\dot{q}_n + \omega_n^2\,q_n = m_n^{-1}\,Q_n \tag{18}$$

Methods for obtaining values of ξ_n from vibration test data are given in the monograph covering that subject. The dissipative forces associated with sloshing are covered in the sloshing model monograph.

3.2 ADDING COMPONENTS USING MODE SYNTHESIS

Frequently it is desirable to make a parameter study to determine the effect on vehicle response resulting from changes in the characteristics of a specific area or component, e.g., a sloshing mass or engine system. Rather than make several analyses of the system changing but a fraction of the parameters each time, the vibration characteristics of the system excluding the specific varying parameter may be calculated, and then modified by coupling the parameter back in through the mode synthesis technique (discussed in Section 4.3).

For reasons developed more fully in Section 4.3, the mode synthesis approach may result in a loss of accuracy. The analysis that considers the most information about the system will be the most accurate. The use of many modes in the mode synthesis technique will give theoretically more accurate results than using a minimum number of modes. This aspect is one which must be handled by discretion born of experience. As an example, in calculating the torsion modes with engine representation, three alternatives are available.

a. Include the engine inertia as an attached spring-inertia to the shaft in the modes calculation.

b. Assume the engine inertia is included in the "rigid" components for modes calculation. The engine elasticity is then included through mode synthesis by adding the single spring mass mode and subtracting the engine inertia effects from the torsion modes. This requires both inertial and elastic coupling in the synthesis.

c. Assume the engine inertia can be eliminated in the "rigid" components for modes calculations. The engine is then included through mode synthesis by adding the simple spring mass mode. This requires only elastic coupling in the synthesis.

These alternatives are listed in order of accuracy of end results following the general rule stated previously. There are many examples where there would be little if any degradation of accuracy. As an example, consider a vehicle with first torsion frequency of 20 cps and first engine frequency of 5 cps, then the engine is essentially uncoupled from the elastic modes. If the engine frequency were 15 cps, then considerable coupling is possible.

Although engines were used as an example, the same is true for any representation of this type, i.e., engines, payloads, or any other large component or specific parameter under investigation.

3.3 CORRECTING MODEL BASED ON TEST RESULTS

The final verification of analytical techniques is a comparison with experimental data. Perfect comparisons are indeed exceptions since both the analytical model and experimental model are approximations to some extent. The analytical approximations have been discussed. The major experimental approximations are centered around suspension system effects and vehicle modifications required to accommodate the suspension system. No general rule can be made to obtain better agreement between test and analytical. Careful examination of the data and the structure will probably indicate several areas where the representation is inadequate or does not define the test speciment. Possible causes of differences are:

a. Effects of suspension system on test environment.

b. Stiffness of joints or trusses.

c. Effect of large components, such as engines.

d. Experimental modes may be impure, i.e., not orthogonal or include parts of other modes.

e. Representation of system inertia.

The work of Reference 7 presents a method for obtaining the flexibility matrix from experimental mode data. The procedure orthogonalizes the experimental modes, using an analytical mass distribution, and then derives the flexibility matrix of the structure. This method can be useful if complete and accurate experimental data is obtained for a system difficult to model. It can also be used to locate possible discrepancies between analytical and experimental results.

3.4 SOLID BOOSTERS

Torsion models of solid propellant vehicles require the same considerations as liquid propellant vehicles except in the treatment of the propellants. All the propellant is included in inertia representation of the solids as compared with complete omission in the case of liquids. Since torsional problems have not been encountered in solid

vehicles, very little work has been done to substantiate the model, analytically or experimentally. It can be inferred from the monograph on longitudinal models that a large portion of the mass can be considered attached to the outer casing. The inner portion could then be considered attached through appropriate springs. However, since effective inertia decreases as the fourth power of the radius, no appreciable error is introduced by assuming the entire mass rigid.

3.5 CLUSTERED BOOSTERS

One method for obtaining the higher thrust required for large payloads is to attach rocket-engines or motors to a central core; for liquid boosters a peripheral ring of propellant tanks is attached to a center tank and the engines are supported on truss members connecting the tanks; for solid boosters, the motors are attached to a central solid or liquid booster. These clustered tank designs destroy axial symmetry and quite often planes of symmetry. This results in a more complicated lateral model where a number of cylindrical tanks are coupled by their elastic connections and must be allowed freedom in several directions for an adequate description of vehicle modes.

For preliminary design it is sufficient to choose approximate planes of symmetry and analyze the vehicle for bending modes in pitch and yaw planes using branch beams connected to the central core by translational and rotational springs. Simplified torsional and longitudinal models will also suffice at this stage. These simple models can be used to identify possible problem areas (such as relative modal frequencies) and provide design criteria for the connections between tanks.

A complete analysis (or test) should be undertaken to describe all the primary modes of the clustered vehicle. This analysis would provide displacement and rotation in two mutually perpendicular planes; torsion and longitudinal motion. The model of the tanks for displacement and rotation in each of the two planes would be very similar to that discussed for the cylindrical booster. Provision must be made to account for the motion of the outer tanks in these two directions due to the torsional displacement of the center tank and the elastic connections. It is also possible that longitudinal motion will couple with lateral and torsional displacement. As an example, consider a cluster arrangement where the connection at the bottom transmits moment, shear, and axial restraints while the connection at the top provides only shear restraint. Then it is possible to find a mode where the external tanks are bending, causing moments and deflections at the connection to the center core which will result in longitudinal motion of the core. The significance of these types of modes can only be ascertained from the analysis (or test) and can vary greatly from vehicle to vehicle.

The torsional properties in the model can be represented by the torsional stiffness and roll inertia of each tank. The tanks must then be connected by the elastic properties of the truss. Formation of the longitudinal model is given in the monograph on that subject. The complete model for the clustered booster then consists of the

lateral model in two planes, the torsional model and the longitudinal model. These models are then combined through the elasticity and geometry of the connections to provide the stiffness and/or mass coupling.

Analysis (or test) will probably show some planes of symmetry and can also show that some of the coupling mechanisms are unimportant for the particular problem to be solved. If this is the case, it is justified, and expedient, to devise a mathematical model from the results of the complete analysis (or test) which represents the modes of interest.

The analytical representation of the clustered booster is more approximate than that of the one-dimensional beam lateral model, especially for the condition of coupled modes. The tri-axial strain relationships are not completely satisfied, and the inertia terms could be poorly represented in the combination lateral-axial motion. These effects generally are of second order and as such should not alter the primary modes. The elasticity of the connection points probably will require test data for accurate values. The numerical techniques employed for the solution of the system characteristics have been used for many years in the industry; however, some problems in accuracy can be encountered when applied to the clustered booster. The number of points describing the system may be compromised for efficient computer operation and this vehicle may have modes of nearly equal frequency which will be difficult to separate analytically (and experimentally).

The elasticity of the vehicle is most easily described by a coupled stiffness matrix, but solving for the characteristics would then involve inversion of this matrix. This inversion may lead to errors because of machine round-off errors. If the inversion is successful, round-off errors could still be significant in the iterations for the characteristic values, especially for modes with nearly equal eigenvalues. The inversion problem can be circumvented by writing the coupled flexibility matrix directly. The required transformations can be complicated and lead to errors, but with special care this is not insurmountable. Another approach would develop an uncoupled flexibility matrix and perform transformations of coordinates to provide all necessary coupling in the mass terms. These last two approaches would still have possible problems in the iterations on the systems characteristics.

An approach useful in calculating modes of complex systems is the component mode synthesis method. Here the modes of the individual pieces are calculated and then the combined modes are obtained from the modes of the component parts. This is based on the assumption that significant motions of the individual tanks can be described by a small number of modes. If this is true, then the solutions for the combined system can be performed in terms of less coordinates.

Most of the clustered booster work to this date has involved two vehicles, the Titan IIIC and the Saturn I. Titan IIIC is comprised of a center core liquid booster with two attached solid boosters (Figure 5); the connections at the bottom transmit

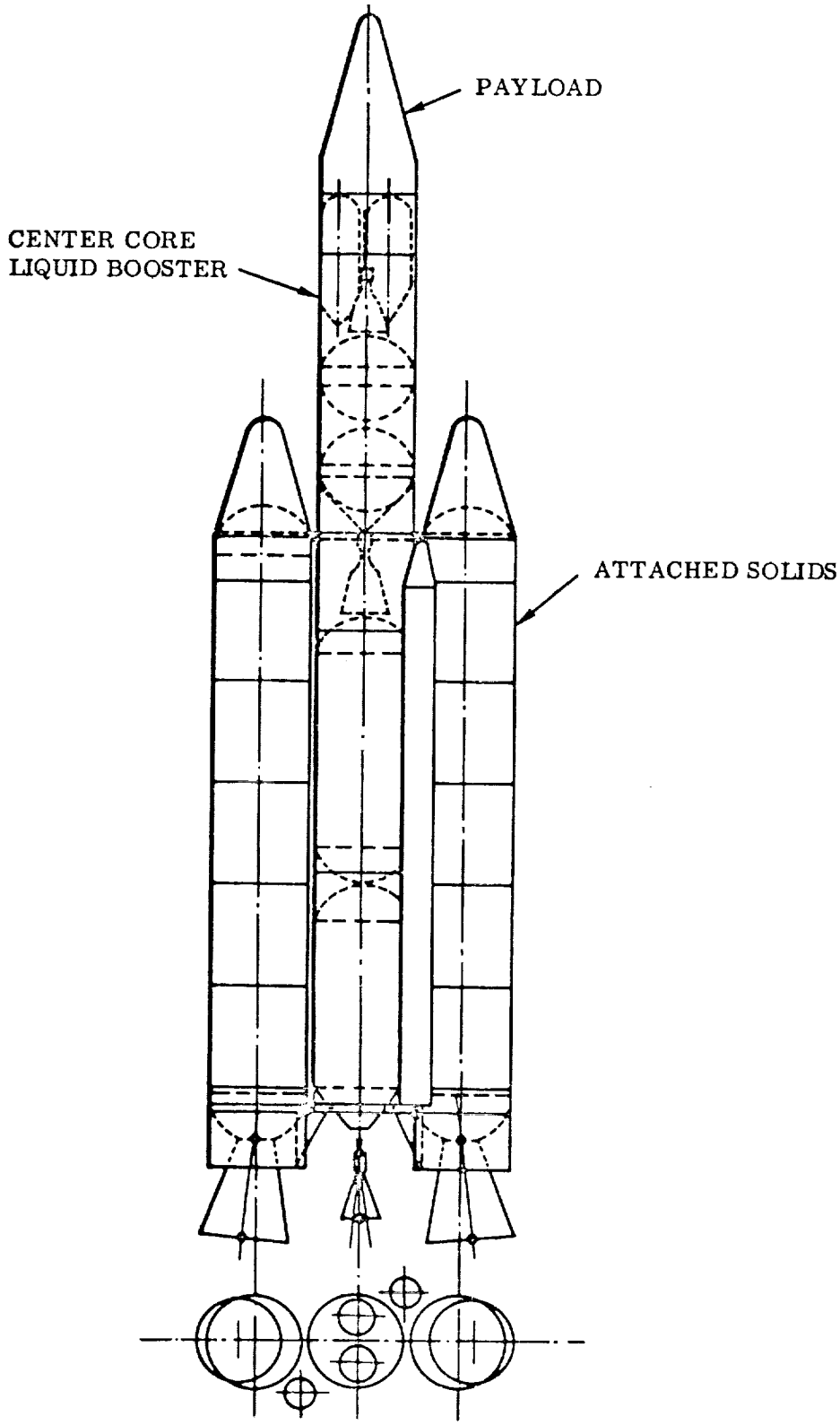

Figure 5. Titan IIIC

axial load, shear, moment, and torque. The top connection transmits only shear. Because of the nature of the connections, it can be seen that yaw bending and longitudinal coupling can occur and pitch bending and torsion is another possible coupling mechanism. Storey in Reference 8 develops the coupled flexibility matrices for these two conditions. This method encountered difficulty in that the number of stations required for adequate representation of the system with the required transformations exceeded computer capacity.

The final Titan IIIC analysis presented in Reference 5 utilizes the mode synthesis approach. The longitudinal, torsional, and pitch and yaw bending modes are determined for each tank and are then coupled by the elasticity of the connecting elements. The influence coefficients for these trusses were obtained experimentally. A report giving comparison of analytical and 1/5 scale experimental results is to be published.

The Saturn I vehicle consists of a center LO_2 tank with eight peripheral tanks for alternating LO_2 and RP-1. These tanks are connected at top and bottom by trusses (Figure 6) providing axial, shear, and torsion restraint in both planes at the bottom plus moment restraint in the tangential planes. The top connection provides similar restraint except for the fuel tanks which do not transmit axial load. The trusses are not symmetric with respect to planes of symmetry of the tanks, but this effect is small so that planes of symmetry as defined by the tanks do not introduce large errors.

Milner (Reference 4) establishes theoretically the uncoupling of pitch, yaw, and torsion modes for a symmetrical clustered booster and investigates the effect of minor asymmetry. Results of this study indicate that the effect of such coupling on natural frequencies is minor; mode shapes are not presented.

Leonis (Reference 9) develops a matrix solution of the dynamics problem of a four-tank booster without center core. The flexibility matrix of the whole unit, with appropriate beam end fixity, is derived. This flexibility matrix together with suitable mass matrix is used to derive equations of free vibration in matrix form. The tanks are assumed to be similar, but the solution can be modified accordingly for the case of nonsimilar tanks and for other tank configurations. The formulation is general so as to furnish any complex mode of vibration. Simple modes, however, can be obtained as particular cases of the general problem.

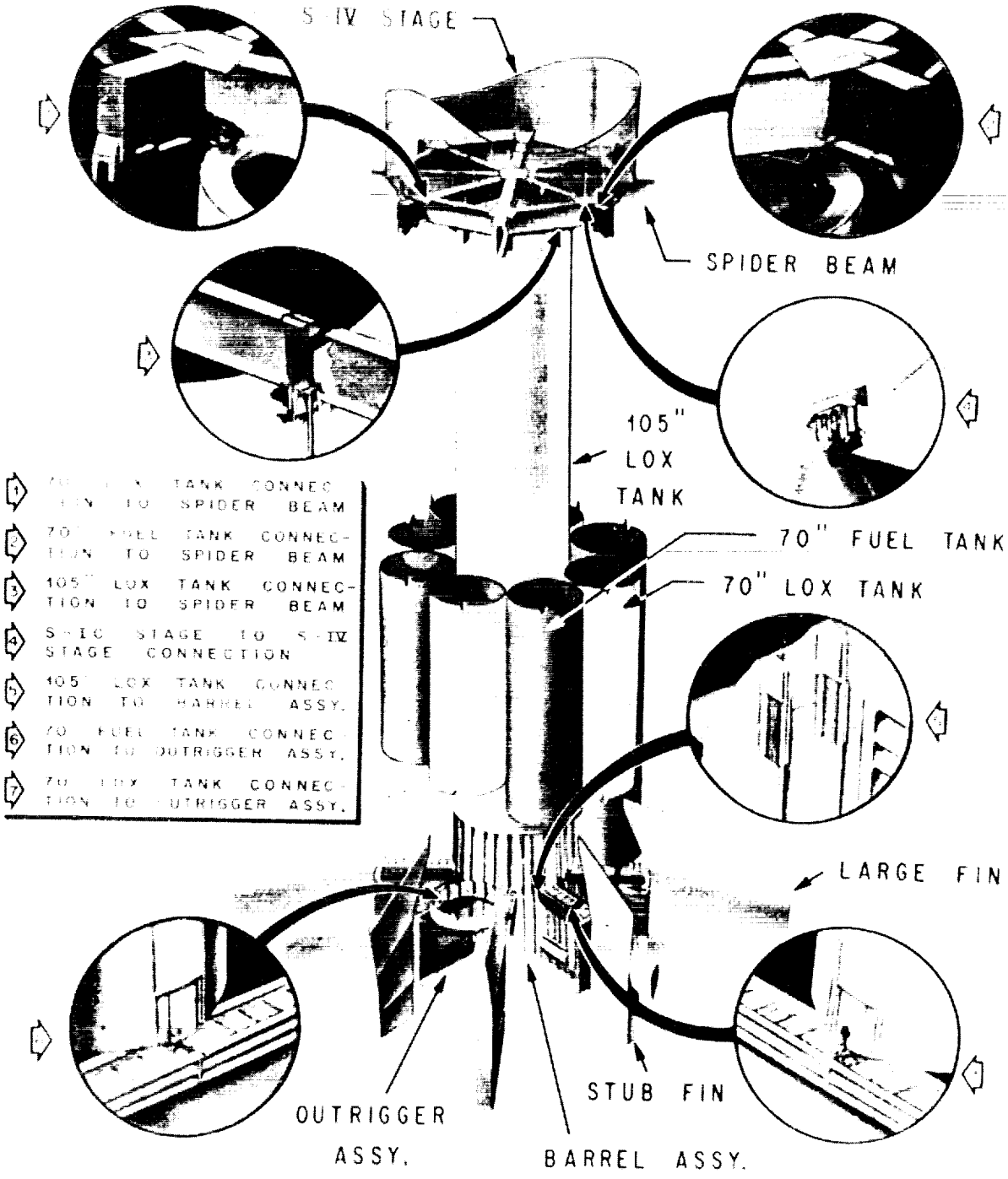

Figure 6. Saturn I Block II Connection Details

4/METHODS FOR SOLUTION

4.1 FORMATION OF THE COUPLED EQUATIONS

The primary purpose of the torsional model is to provide an analogy of the real system which can be represented mathematically. The general approach to the solution of the governing equations, as outlined in Section 3, requires the formation of the inertia, stiffness and dynamic matrices.

4.1.1 STIFFNESS MATRIX. Formation of the dynamic matrix in Equation 10 requires the development of the inertia matrix and the inverse of the stiffness matrix. Direct formation of the flexibility matrix (which is the inverse of the stiffness matrix) is rarely justified. A torsional model is a close-coupled system, i.e., internal forces on one inertia element are dependent on the displacements of adjacent inertia elements only, as opposed to the lateral beam bending model which is far-coupled, i.e., internal forces at a given point may reflect displacements of non-adjacent points.

An element, K_{ij} , of a stiffness matrix may be thought of as the force applied at point i due to a unit displacement at point j when all coordinates of the system other than j are restrained against displacement.

From this definition, it is apparent that it is possible to form the stiffness matrix directly from the spring rates of the system. For example, consider the complex torsional model of Figure 7.

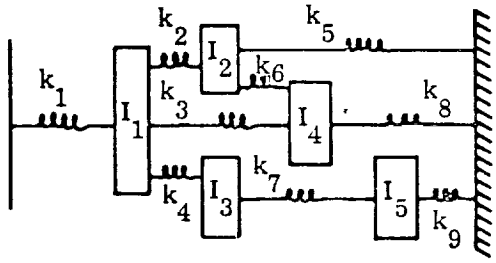

Figure 7. Complex Torsional System

Restraining coordinates 2 through 5 and displacing coordinate 1 a unit amount, the resultant forces will be $(k_1 + k_2 + k_3 + k_4)$ on inertia I_1, $-k_2$ on inertia I_2, $-k_3$ on inertia I_4, and $-k_4$ on inertia I_3. The first row of the stiffness matrix is

$$([k_1 + k_2 + k_3 + k_4] \quad -k_2 \quad -k_4 \quad -k_3 \quad 0)$$

The succeeding rows can be developed in a similar manner. The final stiffness matrix is

$$\begin{bmatrix} (k_1 + k_2 + k_3 + k_4) & -k_2 & -k_4 & -k_3 & 0 \\ -k_2 & (k_2 + k_5 + k_6) & 0 & -k6 & 0 \\ -k_4 & 0 & (k_4 + k_7) & 0 & -k_7 \\ -k_3 & -k_6 & 0 & (k_3 + k_6 + k_8) & 0 \\ 0 & 0 & -k_7 & 0 & (k_7 + k_9) \end{bmatrix}$$

In all cases of pure torsion, it is possible to translate the real system into a model of mass inertias connected by linear torsional springs.

The polar moment of inertia, J, of the vehicle will, most likely, be variable along the vehicle length. This will affect the torsional stiffness. Generally, however, the distribution of polar moment of inertia along the vehicle axis may be idealized with satisfactory accuracy by a straight line segmented curve. Equivalent torsional stiffness may be developed by considering a shaft fixed at one end with a linear variation of J from J_1 to J_2, as shown in Figure 8.

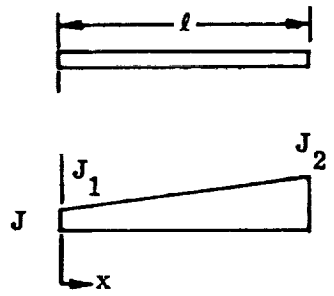

Figure 8. Cantilevered, Linearily Varying Stiffness Beam

The angular twist produced by a torque applied at the free end is given by:

$$\theta = \int_0^{\ell} \frac{T\,dx}{J(x)\,G}$$

where $J(x) = J_1\left[1 + \frac{x}{\ell}\left(\frac{J_2}{J_1} - 1\right)\right]$

or

$$\theta = \frac{T}{GJ_1} \int_0^{\ell} \frac{dx}{1 + \frac{x}{\ell}\left(\frac{J_2}{J_1} - 1\right)}$$

$$= \frac{T}{G\,J_1}\left[\frac{\ell J_1}{J_2 - J_1} \ln\left(1 + \frac{x}{\ell}\left\{\frac{J_2}{J_1} - 1\right\}\right)\right]_0^{\ell}$$

$$= \frac{T}{G}\left[\frac{\ell}{J_2 - J_1}\right] \ln\left(\frac{J_2}{J_1}\right) \qquad (19)$$

The torsional stiffness, k, is equivalent to the torque required to produce a unit twist, or

$$k = \frac{G\,(J_2 - J_1)}{\ell \ln\,(J_2/J_1)} \tag{20}$$

Note that this expression becomes an indeterminate form when $J_1 = J_2$.

However, by employing L'Hospital's rule $\left(\lim_{J \to C} \frac{f(J)}{g(J)} = \frac{\lim_{J \to C} f(J)}{\lim_{J \to C} g(J)} = \frac{\lim_{J \to C} f'(J)}{\lim_{J \to C} g'(J)} \right)$,

a value of k at $J_1 = J_2$ can be found:

$$\frac{d}{d J_1}\left(G\,[J_2 - J_1]\right) = -G$$

$$\frac{d}{d J_1}\left(\ell \ln\,[J_2/J_1]\right) = -\frac{\ell}{J_1}$$

$$\lim_{J_1 \to J_2}\left(\frac{G\,[J_2 - J_1]}{\ell \ln\,[J_2/J_1]}\right) = \frac{\lim_{J_1 \to J_2}\left(G\,[J_2 - J_1]\right)}{\lim_{J_1 \to J_2}\left(\ell \ln\,[J_2/J_1]\right)}$$

$$= \frac{\lim_{J_1 \to J_2} -G}{\lim_{J_1 \to J_2} -\frac{\ell}{J_1}} = \frac{GJ_2}{\ell}$$

Examination of the expression for k indicates that the direction from J_1 to J_2 has no influence on the spring rate. Therefore, if the stipulation is made that $J_2 \geq J_1$, the graph in Figure 9 provides a coefficient to be applied to the stiffness value of the shaft of constant $J = J_2$ to obtain the equivalent spring stiffness of a linearly varying stiffness shaft.

It should be further pointed out that the value of J should never go to zero, as this implies no resistance to torque and, consequently a stiffness value of zero.

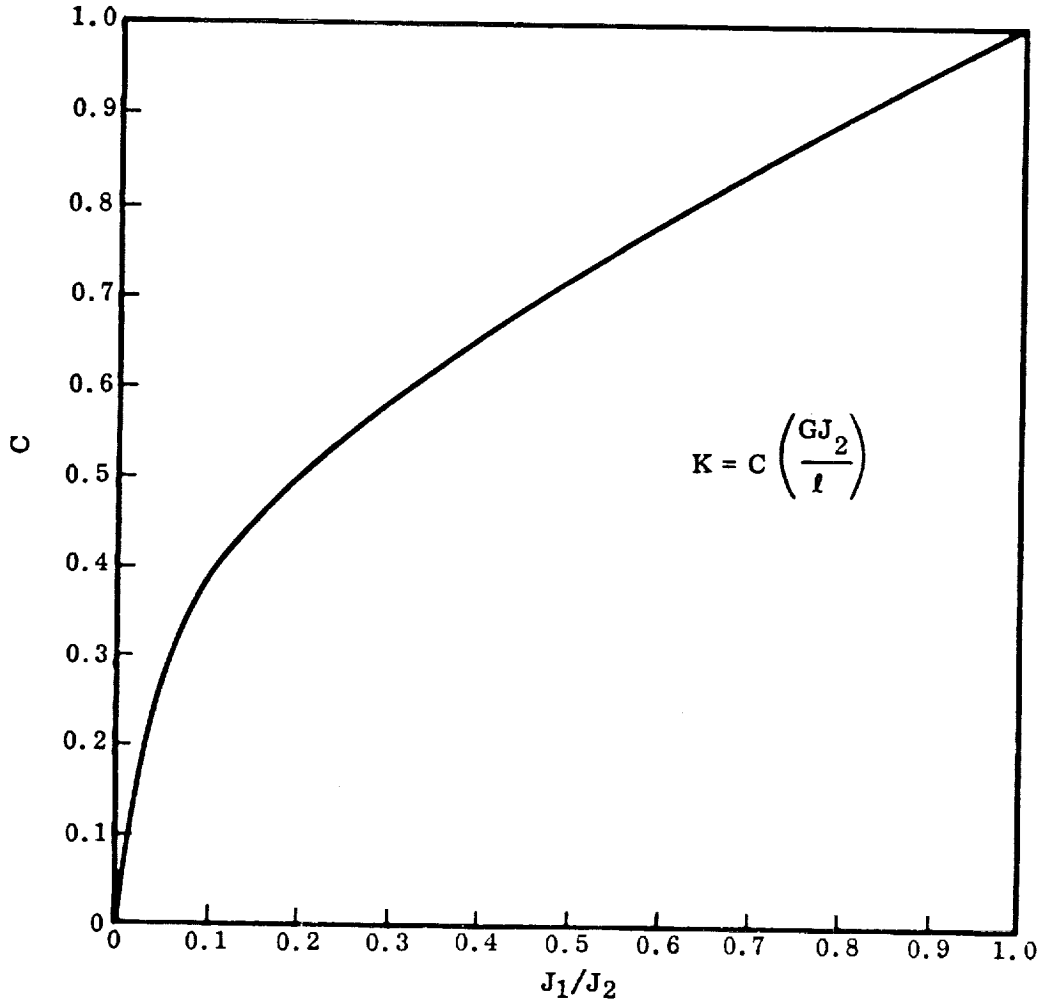

Figure 9. Coefficient of Equivalent Stiffness – Linearly Varying Stiffness Shaft

A tacit assumption of the foregoing discussion is that the model is fixed or connected to at least one point of a rigid, immovable base.

The governing matrix equation in such a case is

$$[M]\{\ddot{\theta}\} + [K]\{\theta\} = 0$$

or, in its solvable form,

$$[C][M]\{\phi\} = \lambda \{\phi\}$$

where $[C]$ is the inverse of the stiffness matrix

$[M]$ is a diagonal matrix of mass inertias

$\{\phi\}$ is the eigenvector to be determined

λ is the eigenvalue to be determined $= 1/\omega^2$

For a free system (one not attached to a rigid base) the form of the equation must be modified to

$$[C][M]\{\phi\} = \lambda [\{\phi\} - \{\alpha\} \upsilon_0] \tag{21}$$

In the analysis of the free system, the structure must be temporarily fixed at one point. If the structure were not fixed, an external moment applied to the system would cause it to rotate uniformly. A solution to the problem would then be impossible. Mathematically, this is represented by a singular stiffness matrix, $[K]$. In Equation 21, the term $-\{\alpha\}\upsilon_0$ releases the fixed point. The resultant rotation is υ_0. By applying the principals of angular momentum to the system, Equation 21 can be expressed as a standard eigenvalue problem

$$\{[C][M]+[TR]\}\{\phi\} = \lambda\{\phi\}$$

where $[TR]\{\phi\} = \lambda\{\alpha\}\upsilon_0$

and $[C][M] + [TR]$ is the final dynamic matrix. The vector $\{\alpha\}$ is a vector whose elements are each 1.

Applying the conservation of angular momentum,

$$I_0 \upsilon_0 + \{\alpha\}'[M]\{\phi\} = 0 \tag{22}$$

where I_0 is the mass inertia at the restrained point.

Premultiply Equation 21 by $\{\alpha\}'[M]$ to obtain

$$\{\alpha\}'[M]\{\phi\} - \{\alpha\}'[M]\{\alpha\}\upsilon_0 = \omega^2\{\alpha\}'[M][C][M]\{\phi\}.$$

Defining

$$\{B\} = \{\alpha\}'[M][C][M],$$

then

$$-I_0\upsilon_0 - \{\alpha\}'[M]\{\alpha\}\upsilon_0 = \omega^2\{B\}\{\phi\}.$$

Since the total vehicle inertia is

$$I_T = I_0 + \{\alpha\}'[M]\{\alpha\},$$

it follows that

$$\upsilon_0 = \frac{\omega^2\{B\}\{\phi\}}{I_T}.$$

By satisfying the identity

$$[TR]\{\phi\} = \lambda\{\alpha\}\upsilon_0$$

it is seen that

$$[TR] = \frac{1}{I_T}\{\alpha\}\{B\} = \frac{1}{I_T}[M][C][M].$$

4.1.2 FLEXIBILITY MATRIX. The simplicity of development of the stiffness matrix for close coupled systems justifies the difficulty of inverting it to form the dynamic matrix in most cases. Forming the flexibility matrix directly is justified only for simpler systems. Virtually any redundancy of the structure makes direct development of the flexibility matrix less practical than inverting the stiffness matrix.

The flexibility matrix relates displacements to applied loads:

$$\{\theta\} = [C]\{M\}$$

Considering each spring element independently

$$\bar{\theta}_i = C_i M_i$$

where $\bar{\theta}_i$ is deformation of one end of the spring with respect to the other end and M_i is the total applied moment. The total deflections of the connected system are found by transforming from relative coordinates to absolute coordinates

$$\{\theta_i\} = [T]\{\bar{\theta}_i\}$$

The total applied loads, M_i, can be considered to be functions of the external moment, m_i, applied to each inertia of the system, expressed by the transformation

$$\{M_i\} = [R]\{m_i\}.$$

Thus the relationship between total displacement, θ_i, and the external moment, m_i, applied to each inertia is developed by substituting the transformed values

$$\{\bar{\theta}_i\} = [C][M_i]$$

$$[T]\{\bar{\theta}_i\} = [T][C][R]\{m_i\}$$

$$\{\theta_i\} = [T][C][R]\{m_i\}.$$

Thus, $[T][C][R] = [C^*]$ equals the coupled flexibility matrix.

For a redundant structure, the influence coefficients are not so readily obtained and use must be made of an appropriate static analysis such as virtual work or Castigliano's theorem, Reference 10.

An example of the development of a flexibility matrix is given below.

Consider the torsional system shown in Figure 10.

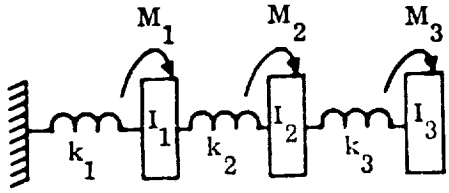

Figure 10. Cantilevered Torsional System

The quantity M_1 is the external torque applied to inertia i. If $C_i = 1/k_i$, the angular deformation of each spring resulting from the total moment imposed on each is given by $\theta_i = C_i M_i$, or for the entire system

$$\begin{Bmatrix} \bar{\theta}_1 \\ \bar{\theta}_2 \\ \bar{\theta}_3 \end{Bmatrix} = \begin{bmatrix} C_1 & 0 & 0 \\ 0 & C_2 & 0 \\ 0 & 0 & C_3 \end{bmatrix} \begin{Bmatrix} M_1 \\ M_2 \\ M_3 \end{Bmatrix} \tag{23}$$

The total deflection of each inertia can be expressed in terms of the relative deformation of the springs,

$$\begin{aligned} \theta_1 &= \bar{\theta}_1 \\ \theta_2 &= \bar{\theta}_1 + \bar{\theta}_2 \\ \theta_3 &= \bar{\theta}_1 + \bar{\theta}_2 + \bar{\theta}_3 \end{aligned}$$

or, in matrix form,

$$\begin{Bmatrix} \theta_1 \\ \theta_2 \\ \theta_3 \end{Bmatrix} = \begin{bmatrix} 1 & 0 & 0 \\ 1 & 1 & 0 \\ 1 & 1 & 1 \end{bmatrix} \begin{Bmatrix} \bar{\theta}_1 \\ \bar{\theta}_2 \\ \bar{\theta}_3 \end{Bmatrix} \tag{24}$$

Combining Equations 23 and 24,

$$\begin{Bmatrix} \theta_1 \\ \theta_2 \\ \theta_3 \end{Bmatrix} = \begin{bmatrix} 1 & 0 & 0 \\ 1 & 1 & 0 \\ 1 & 1 & 1 \end{bmatrix} \begin{bmatrix} C_1 & 0 & 0 \\ 0 & C_2 & 0 \\ 0 & 0 & C_3 \end{bmatrix} \begin{Bmatrix} M_1 \\ M_2 \\ M_3 \end{Bmatrix}$$

or

$$\begin{Bmatrix} \theta_1 \\ \theta_2 \\ \theta_3 \end{Bmatrix} = \begin{bmatrix} C_1 & 0 & 0 \\ C_1 & C_2 & 0 \\ C_1 & C_2 & C_3 \end{bmatrix} \begin{Bmatrix} M_1 \\ M_2 \\ M_3 \end{Bmatrix} \tag{25}$$

The total moment at any element can be related to the applied loads at each point

$$M_1 = m_1 + m_2 + m_3$$

$$M_2 = m_2 + m_3$$

$$M_3 = m_3$$

or, in matrix form,

$$\begin{Bmatrix} M_1 \\ M_2 \\ M_3 \end{Bmatrix} = \begin{bmatrix} 1 & 1 & 1 \\ 0 & 1 & 1 \\ 0 & 0 & 1 \end{bmatrix} \begin{Bmatrix} m_1 \\ m_2 \\ m_3 \end{Bmatrix} \tag{26}$$

Substituting Equation 26 into Equation 25 yields

$$\begin{Bmatrix} \theta_1 \\ \theta_2 \\ \theta_3 \end{Bmatrix} = \begin{bmatrix} C_1 & 0 & 0 \\ C_1 & C_2 & 0 \\ C_1 & C_2 & C_3 \end{bmatrix} \begin{bmatrix} 1 & 1 & 1 \\ 0 & 1 & 1 \\ 0 & 0 & 1 \end{bmatrix} \begin{Bmatrix} m_1 \\ m_2 \\ m_3 \end{Bmatrix}$$

or

$$\begin{Bmatrix} \theta_1 \\ \theta_2 \\ \theta_3 \end{Bmatrix} = \begin{bmatrix} C_1 & C_1 & C_1 \\ C_1 & (C_1+C_2) & (C_1+C_2) \\ C_1 & (C_1+C_2) & (C_1+C_2+C_3) \end{bmatrix} \begin{Bmatrix} m_1 \\ m_2 \\ m_3 \end{Bmatrix}$$

4.1.3 TRANSFORMED MASS MATRIX. An approach that is particularly advantageous for close-coupled systems is that of transforming the coordinate system from the absolute to the relative sense. In prior discussions the displacements of the system coordinates have been referenced to a fixed point or neutral position. These same displacements may also be expressed relatively; referenced to an adjacent coordinate. The relationship between displacements in absolute terms, $\{\theta\}$, and the displacements in relative terms, $\{\bar{\theta}\}$, is readily described by a simple transformation matrix:

$$\{\theta\} = [T]\ \{\bar{\theta}\}$$

Thus the kinetic energy of the system can be expressed in terms of relative coordinates by

$$2KE = \{\dot{\bar{\theta}}\}' [T]' [M][T]\{\dot{\bar{\theta}}\}$$

The deflections of the connecting springs are expressed in terms of relative coordinates, which, in its most general form requires another transformation matrix

$$\{\Delta\} = [TR]\{\bar{\theta}\}$$

If the number of springs is equal to or less than the number of inertias, the deflection of each spring will be defined by a different relative displacement; consequently the transformation matrix, [TR], can be written as a diagonal matrix of unit elements. For such a case, [TR]may be neglected without affecting the solution.

The potential energy of the system is given by

$$2PE = \{\bar{\theta}\}[TR]'[K][TR]\{\bar{\theta}\}$$

where K is a diagonal matrix of the spring rates.

Substituting the kinetic energy and potential energy terms into LaGrange's equation

$$\frac{d}{dt}\left[\frac{\partial(KE)}{\partial \dot{q}_i}\right] + \frac{\partial PE}{\partial q_i} + \frac{\partial W}{\partial q_i} = 0$$

the equations of motion become

$$[T]'[M][T]\{\ddot{\bar{\theta}}\} + [TR]'[K][TR]\{\bar{\theta}\} = 0$$

and the dynamic matrix is established by

$$[([TR]'[K][TR)^{-1}[T]'[M][T]]\{\phi\} = \lambda\{\phi\}$$

The advantages of this method are greatest when the system is free or cantilevered and multiple load paths are absent or constitute only a minor portion of the system. Under these conditions, the transform matrix [TR]contains little or no off-diagonal terms; the matrix [TR]'[K][TR] is no more than slightly coupled and may be inverted with a minimum of effort.

When the number of springs is equal to or less than the number of inertias, the transform matrix is a diagonal matrix of unit elements; [TR]'[K][TR] reduces to [K] which, being a diagonal matrix, can be immediately inverted by taking the reciprocals of the individual elements of the diagonal. The dynamic matrix can be determined with a minimum of effort and operated on to obtain modal data.

This approach is very similar to the method in the previous section with the transformation of coordinates coupling the mass matrix instead of the flexibility matrix. Note that the modes, $\{ \phi \}$, are in terms of relative coordinates and must be premultiplied by the transform matrix, $[T]$, to obtain absolute vectors.

4.2 SOLUTIONS FOR CHARACTERISTICS

Formulation of the equations of motion of dynamic systems results in a linear differential equation for the continuous exact solution or a series of differential equations for the approximate solutions. For torsional vibration usually only the lower modes are of any significance and therefore the approximate solutions are of practical importance. Two methods are used to describe the system in these approximate solutions: 1) the system is divided into a finite number of segments connected by massless stiffness, and 2) the system is described in terms of assumed functions. Solving for the characteristics of the resulting equations can be categorized into three groups. These are 1) energy methods, 2) solving the differential equation and 3) solving the integral equation. The equations are in the general matrix form

$$- \omega^2 [M] \{ \theta \} + [K] \{ \theta \} = 0 \quad \text{(differential equation)} \tag{27}$$

or

$$\{ \theta \} = \omega^2 [K]^{-1} [M] \{ \theta \} = 0 \quad \text{(integral equation)} \tag{28}$$

The most general solution of Equation 27 involves expansion of the determinant and solving the polynomial equation. This procedure is adequate for simple systems and up to four degrees of freedom can be solved easily. Methods for higher order systems have been developed in References 11 and 12. However, since only the lower modes are important, some approximate methods have been developed which obtain these modes and frequencies with sufficient accuracy. As a matter of convenience, many of these methods are discussed in some detail in the monograph on lateral modes or can be found in Reference 13.

4.2.1 MATRIX ITERATION. (Stodola and Vianello Method). The matrix iteration technique is essentially the Stodola and Vianello method in matrix form. This method was developed by Stodola (Reference 14) primarily for application to turbine rotors.

4.2.2 HOLZER (MYKLESTAD). A useful and practical method of determining mode shapes and frequencies known as the Holzer method has been used by many engineers for years. It was developed by Holzer (Reference 15) primarily for torsional problems and extended by Myklestad (Reference 16) to the beam bending problem.

4.2.3 ENERGY METHODS (RAYLEIGH-RITZ). Lord Rayleigh's method of evaluating the fundamental frequency of a system is based on the principle of conservation of

energy. At the maximum deformation of the system vibrating at its fundamental frequency, all the energy of the system is in a potential energy form $\left(PE = \frac{1}{2}\int JG\left(\frac{d\theta}{dx}\right)^2 dx\right)$. But at the instant the system passes through the equilibrium position, its energy is entirely in kinetic form ($KE = \frac{1}{2}\int I\dot{\theta}^2 dx$). If energy is conserved, the maximums of those two values may be equated. This criterion was first mentioned by Lord Rayleigh in 1877 (Reference 17).

4.2.4 MODAL QUANTITIES. Solutions to the characteristic equations give the reciprocals of the squares of the circular frequencies and also the mode shapes of the restrained system. The linear frequencies of vibration are obtained from the circular frequencies. If each mode shape, $\{\phi_n\}$, is considered to be the n^{th} column of a matrix $[\Phi]$ of all the mode shapes, then $[\Phi]'[M][\Phi]$ is an orthogonality check of the mode shapes. The diagonal element, $([\Phi]'[M][\Phi])_{nn}$, is called the generalized inertia of the system for the mode n. (The generalized inertia of the system may be considered to be a measure of the kinetic energy of the system.) In this discussion the vector $\{\phi\}$ was stated to be a mode shape of the structural system. For a restrained system, $\{\phi\}$ is the complete mode shape. For a free-free system the displacements due to υ_0 must be added to obtain the complete mode shape. Also, for a free-free system, the generalized inertia must be modified to include the contribution of the temporarily fixed point.

4.3 MODE SYNTHESIS ANALYSIS

The complicating aspects of the clustered booster vehicle have, as a net effect, the requirement of large numbers of coordinates in the model. The resultant size of the governing equations may well be so large as to overwhelm the best of analysts or computers. The technique of modal synthesis is a process whereby the dynamic characteristics of the several components of the system are calculated separately, and then brought together to evaluate the dynamic characteristics of the entire system. (This is discussed in some detail in the monograph on lateral mode.)

4.4 EXAMPLE OF COUPLED BENDING-TORSION ANALYSIS

To illustrate the procedures used in a coupled bending-torsion analysis, the system of Figure 11 will be analyzed using the stiffness matrix and mode synthesis approaches. The procedure using the flexibility matrix approach is given in References 8 and 9.

The system consists of three uniform tanks, BE, CF, and DG. The center tank, CF, continues to a fixed base A through structure CA which has the same structural properties as the tank but has no mass. The outer tanks BE and DG are connected to the center tank CF by crossbeams EFG and BCD and lateral springs, k. The crossbeams are rigidly attached to the center tank and pinned with ball joints at the outer tanks. It is assumed that the crossbeams are rigid in the y-direction;

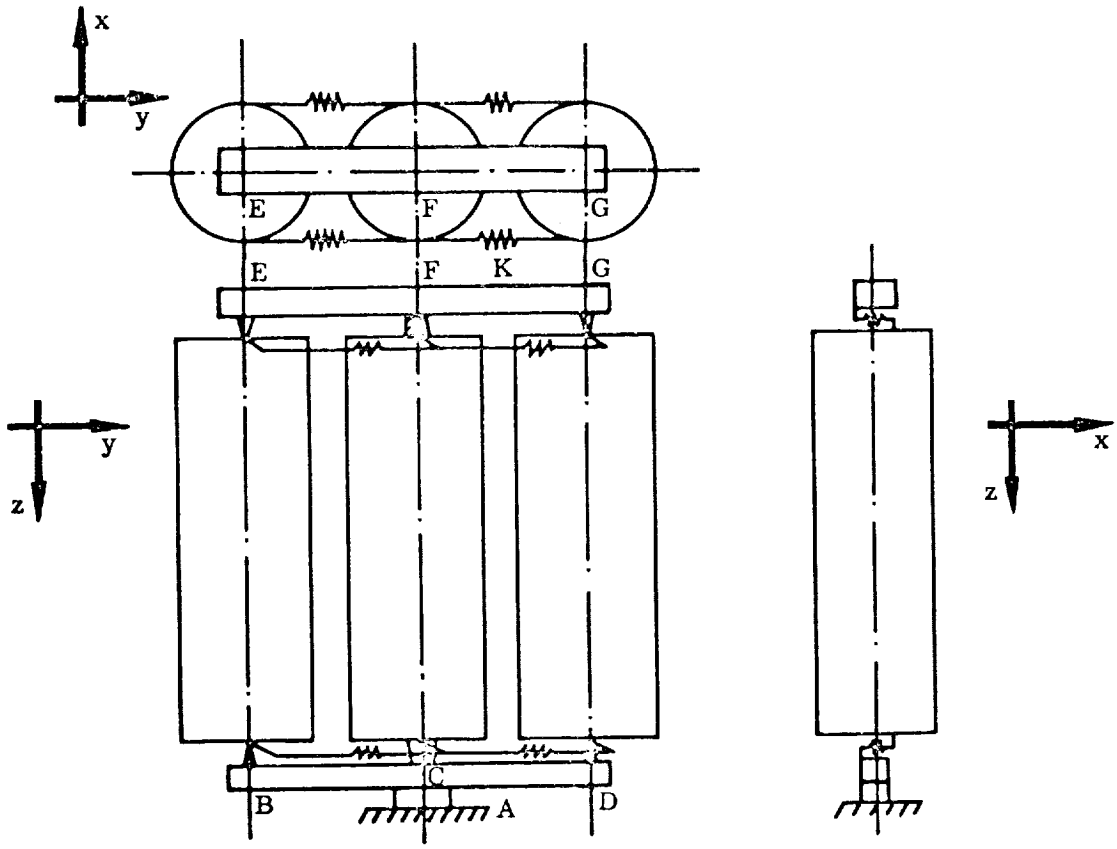

Figure 11. Sample Bending Torsion System

therefore, the lateral springs, k, act only as torsional springs. The system was constructed in this manner so that for purposes of an example problem, the coupling is restricted to torsion about the Z axis and bending in the X-Z plane. Also, to shorten the problem, rotary inertia in bending was assumed to be equal to zero.

This system is represented by the lumped model of Figure 12. The mass and inertia are lumped at twelve equally spaced stations. Stations 1, 4, 5, 8, 9, and 12 each have 1/6 of the tank mass or inertia. Stations 2, 3, 6, 7, 10, and 11 each have 1/3 of the tank mass or inertia. The lateral springs k are replaced by an equivalent torsion spring, D. A lateral spring, E, connects the crossbeam and outer tank (representing the lateral stiffness of the ball joint).

4.4.1 STIFFNESS MATRIX SOLUTION. The typical beam element stiffness is given below (shear stiffness effects are not included).

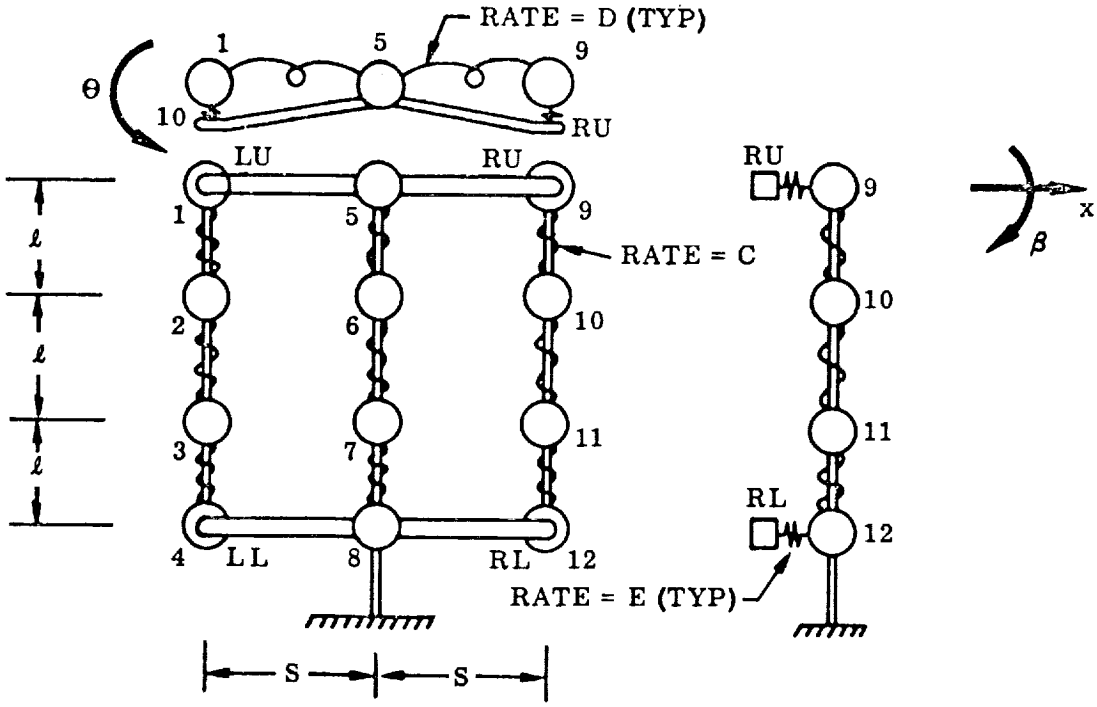

Figure 12. Analytical Model of Sample System

$$\frac{[K_{beam}]\{X\}}{\frac{12EI}{\ell^3}} = \begin{bmatrix} 1 & -1 & -\frac{\ell}{2} & -\frac{\ell}{2} \\ -1 & 1 & \frac{\ell}{2} & \frac{\ell}{2} \\ -\frac{\ell}{2} & \frac{\ell}{2} & \frac{\ell^2}{3} & \frac{\ell^2}{6} \\ -\frac{\ell}{2} & \frac{\ell}{2} & \frac{\ell^2}{6} & \frac{\ell^2}{3} \end{bmatrix} \begin{Bmatrix} X_i \\ X_{i+1} \\ \beta_i \\ \beta_{i+1} \end{Bmatrix}$$

(Example shown is for vertical beam. For lateral beam, replace ℓ with S)

There will be ten such matrices for the vertical beams, and four for the lateral beams. It should be noted that these 4×4 beam matrices are direction-dependent; i.e., the direction from node i to i + 1 must be the same for all vertical beam segments, and the same for all lateral beam segments. In addition, there will be ten 2×2 torsional stiffness matrices for the vertical beams, four torsional stiffness matrices for the lateral clock-springs; four 2×2 stiffness matrices reflect the linear springs at the ends of the outer beam. These 32 individual element matrices are combined into one overall stiffness matrix as directed in Reference 8, or the monograph on lateral models. This unrestrained stiffness matrix is reduced, partitioned, and reordered according to the reference. The diagonal mass matrix associated with the reduced stiffness matrix can be formed directly. The stiffness matrix is inverted, and post multiplied by the mass matrix to form the dynamic matrix, which is then iterated upon to determine the eigenvalues and eigenvectors.

4.4.2 MODE SYNTHESIS SOLUTION. For the mode synthesis approach, the structure is divided into smaller components of simple construction. Torsion and bending of individual beams can be considered uncoupled; consequently, the torsional model and the bending model for each beam can be represented separately. Separation of the elements is accomplished by removing the lateral beams and springs.

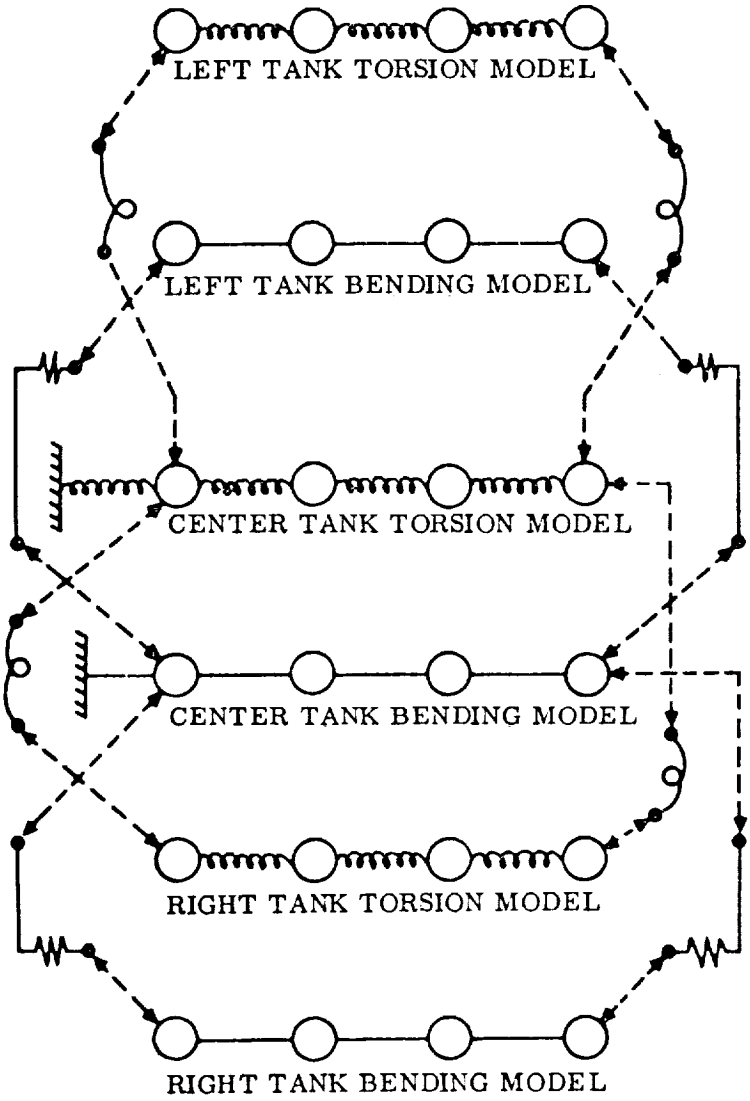

Figure 13. Separation of Model Into Components

As is demonstrated in Reference 8, or Section 4.3 above, the final governing equation is

$$[\mathfrak{m}]\{\ddot{\eta}\} + \left[[\omega^2\mathfrak{m}] + [TS]'[RC]'[K_c][RC][TS]\right]\{\eta\} = 0 \quad (29)$$

where $[\mathfrak{m}]$ is a diagonal matrix of the generalized masses (or generalized inertias) of the component modes, both rigid body and elastic; $[\omega^2\mathfrak{m}]$ is a diagonal matrix of the products of circular frequency squared and generalized mass of each component mode; $[TS]$ is a transformation matrix relating coordinate displacements to modal weighting factors: $\{X\} = [TS]\{\eta\}$; $[RC]$ is a transformation matrix relating connecting element deformations to coordinate displacements: $\{\Delta\} = [RC]\{X\}$; $[K_c]$ is a matrix of connecting element stiffnesses; and $\{\eta\}$ is a vector of modal weighting factors.

For the left hand tank, let X_L represent the weighting factor for its rigid body translation, β_L the rigid body rotation, Θ_L the rigid body torsional rotation, Φ_{BL} the matrix of elastic bending mode shapes, and Φ_{TL} the matrix of elastic torsional mode shapes. Also η_{iBL} and η_{jTL} represent the modal weighting factors for the i^{th} elastic bending mode and j^{th} elastic torsional mode. Similar quantities, where appropriate, can be established for the other tanks simply by replacing the L in the subscripts with a C or R. The transform matrix $[TS]$ is thus:

$$\begin{Bmatrix} X_1 \\ X_2 \\ X_3 \\ X_4 \\ \hline X_5 \\ X_6 \\ X_7 \\ X_8 \\ \hline X_9 \\ X_{10} \\ X_{11} \\ X_{12} \\ \hline \theta_1 \\ \theta_2 \end{Bmatrix} = \left[\begin{array}{ccccccccccc} 1 & \frac{3\ell}{2} & & & & & & & & & \\ 1 & \frac{\ell}{2} & \Phi_{BL} & 0 & 0 & 0 & 0 & 0 & 0 & 0 & 0 \\ 1 & -\frac{\ell}{2} & & & & & & & & & \\ 1 & -\frac{3\ell}{2} & & & & & & & & & \\ \hline & & & & & & & & & & \\ 0 & & 0 & 0 & 0 & \Phi_{BC} & 0 & 0 & 0 & 0 & 0 \\ & & & & & & & & & & \\ & & & & & & & & & & \\ \hline & & & & & & & 1 & \frac{3\ell}{2} & & \\ 0 & & 0 & 0 & 0 & 0 & 0 & 1 & \frac{\ell}{2} & \Phi_{BR} & 0 \quad 0 \\ & & & & & & & 1 & -\frac{\ell}{2} & & \\ & & & & & & & 1 & -\frac{3\ell}{2} & & \\ \hline & & & 1 & & & & & & & \\ 0 & & 0 & 1 & \Phi_{TL} & 0 & 0 & 0 & 0 & 0 & 0 \end{array}\right] \begin{Bmatrix} X_L \\ \beta_L \\ \eta_{1BL} \\ \eta_{2BL} \\ \Theta_L \\ \eta_{1TL} \\ \eta_{2TL} \\ \eta_{3TL} \\ \eta_{1BC} \\ \eta_{2BC} \\ \eta_{3BC} \\ \eta_{4BC} \\ \eta_{1TC} \\ \eta_{2TC} \end{Bmatrix}$$

Transformation Matrix, Contd.

$$
\begin{bmatrix} \theta_3 \\ \theta_4 \\ \theta_5 \\ \theta_6 \\ \theta_7 \\ \theta_8 \\ \theta_9 \\ \theta_{10} \\ \theta_{11} \\ \theta_{12} \end{bmatrix}
=
\begin{bmatrix}
 & & 1 & & & & & & & \\
 & & 1 & & & & & & & \\
\hline
0 & 0 & 0 & 0 & 0 & \Phi_{TC} & 0 & 0 & 0 & 0 \\
 & & & & & & & & & \\
 & & & & & & & & & \\
\hline
 & & & & & & & 1 & & \\
0 & 0 & 0 & 0 & 0 & 0 & 0 & 1 & \Phi_{TR} & \\
 & & & & & & & 1 & & \\
 & & & & & & & 1 & &
\end{bmatrix}
\begin{bmatrix} \eta_{3TC} \\ \eta_{4TC} \\ X_R \\ \beta_R \\ \eta_{1BR} \\ \eta_{2BR} \\ \Theta_R \\ \eta_{1TR} \\ \eta_{2TR} \\ \eta_{3TR} \end{bmatrix}
$$

The deformation of the connecting springs is expressed in terms of coordinate deflections, via another transformation matrix, [RC]:

$$
\begin{Bmatrix} \Delta X_{1-5} \\ \Delta X_{4-8} \\ \Delta X_{9-5} \\ \Delta X_{12-8} \\ \Delta\theta_{1-5} \\ \Delta\theta_{4-8} \\ \Delta\theta_{9-5} \\ \Delta\theta_{12-8} \end{Bmatrix}
=
\begin{bmatrix}
1000 & -1000 & & & & S000 & \\
0001 & 000-1 & & & & 000S & \\
\hline
 & -1000 & 1000 & & & -S000 & \\
 & 000-1 & 0001 & & & 000-S & \\
\hline
 & & & 1000 & -1000 & & \\
 & & & 0001 & 000-1 & & \\
\hline
 & & & & -1000 & 1000 & \\
 & & & & 000-1 & 0001 &
\end{bmatrix}
\begin{Bmatrix} X_1 \\ \vdots \\ X_{12} \\ \theta_1 \\ \vdots \\ \theta_{12} \end{Bmatrix}
$$

where S is the lateral distances between beams.

In this particular case, the connecting elements are simple spring elements, thus simplifying the connecting stiffness matrix, $[K_C]$, to a diagonal matrix. (The lateral beams and translational springs between them and the outer tanks are combined into an equivalent linear spring.)

The governing equation, Equation 29, can now be formed. Eigenvalues and eigenvectors are obtained; however, the eigenvectors must be premultiplied by the coordinate transform matrix [TS] to obtain mode shapes in terms of the original coordinate system.

4.4.3 COMPARISON OF SOLUTIONS. To compare the results of these two methods of analysis, it is necessary to substitute numerical values. For this sample, the following parameters were used:

a. Vertical beams:

ℓ	=	10 m
EI_{yy}	=	10^9 n-m^2
$m_{1, 4, 5, 8, 9, 12}$	=	4,325 kg
$m_{2, 3, 6, 7, 10, 11}$	=	8,650 kg
equivalent $k_{TORSION}$	=	5.92×10^7 n-m/rad
$I_{1, 4, 5, 8, 9, 12}$	=	0.8×10^4 kg-m^2
$I_{2, 3, 6, 7, 10, 11}$	=	1.6×10^4 kg-m^2

b. Lateral beams:

S	=	3 m
EI_{xx}	=	1.6×10^6 n-m^2

c. Connecting elements:

lateral torsion spring rate = D = 10^8 n-m/rad

ball joint translational spring rate = 7.8×10^8 n/m

The unrestrained stiffness matrix was constructed as shown below. It is arranged so as to present the coordinates associated with masses and inertias (X_i, θ_i) first, followed by those coordinates which are not associated with masses and inertias (β_i, X_{LU}, X_{LL}, X_{RU}, X_{RL}, θ_{LU}, θ_{LL}, θ_{RU}, θ_{RL}), and finally those coordinates where motion is restrained (X_A, θ_A, β_A). By arranging the coordinates in this fashion, the resultant matrix needs no reordering and may be reduced by partitioning immediately.

Unrestrained Stiffness Matrix

	$X_1 \cdots X_{12}$		$\theta_1 \cdots \theta_{12}$		$\beta_1 \cdots \beta_{12}$		X_{LU}	X_{LL}	X_{RU}	X_{RL}	θ_{LU}	θ_{LL}	θ_{RU}	θ_{RL}	X_A	θ_A	β_A
$X_1 \vdots X_{12}$	1	12	13	24	25	36	37	38	39	40	41	42	43	44	45	46	47
$\theta_1 \vdots \theta_{12}$	13	24															
$\beta_1 \vdots \beta_{12}$	25	36															
X_{LU}	37																
X_{LL}	38																
X_{RU}	39																
X_{RL}	40																
θ_{LU}	41																
θ_{LL}	42																
θ_{RU}	43																
θ_{RL}	44																
X_A	45																
θ_A	46																
β_A	47																

Table 2. Non-zero Elements of the Upper Triangle of the Sample Coupled System Unrestrained Stiffness Matrix

ROW	COLUMN	ALGEBRAIC VALUE	NUMERIC VALUE
1	1	A + E	7.92×10^8
1	2	-A	-12×10^6
2	2	2A	24×10^6
2	3	-A	-12×10^6
3	3	2A	24×10^6
3	4	-A	-12×10^6
4	4	A + E	7.92×10^8
5	5	A + 2B	1.3422×10^7
5	6	-A	-12×10^6
6	6	2A	24×10^6
6	7	-A	-12×10^6
7	7	2A	24×10^6
7	8	-A	-12×10^6
8	8	2A + 2B	2.5422×10^7
9	9	A + E	7.92×10^8
9	10	-A	-12×10^6
10	10	2A	24×10^6
10	11	-A	-12×10^6
11	11	2A	24×10^6
11	12	-A	-12×10^6
12	12	A + E	7.92×10^8
13	13	C + D	1.592×10^8
13	14	-C	-5.92×10^7
14	14	2C	1.184×10^8
14	15	-C	-5.92×10^7
15	15	2C	1.184×10^8

Table 2. Non-zero Elements of the Upper Triangle of the Sampled Coupled System Unrestrained Stiffness Matrix, Contd.

ROW	COLUMN	ALGEBRAIC VALUE	NUMERIC VALUE
15	16	$-C$	-5.92×10^7
16	16	$C + D$	1.592×10^8
17	17	$C + 2D + 2/3\ BS^2$	2.63466×10^8
17	18	$-C$	-5.92×10^7
18	18	$2C$	1.184×10^8
18	19	$-C$	-5.92×10^7
19	19	$2C$	1.184×10^8
19	20	$-C$	-5.92×10^7
20	20	$2C + 2D + 2/3\ BS^2$	3.22666×10^8
21	21	$C + D$	-1.592×10^8
21	22	$-C$	-5.92×10^7
22	22	$2C$	1.184×10^8
22	23	$-C$	-5.92×10^7
23	23	$2C$	1.184×10^8
23	24	$-C$	-5.92×10^7
24	24	$C + D$	1.592×10^8
25	25	$1/3\ A\ell^2$	4×10^8
25	26	$1/6\ A\ell^2$	2×10^8
26	26	$2/3\ A\ell^2$	8×10^8
26	27	$1/6\ A\ell^2$	2×10^8
27	27	$2/3\ A\ell^2$	8×10^8
27	28	$1/6\ A\ell^2$	2×10^8
28	28	$1/3\ A\ell^2$	4×10^8
29	29	$1/3\ A\ell^2$	4×10^8
29	30	$1/6\ A\ell^2$	2×10^8
30	30	$2/3\ A\ell^2$	8×10^8
30	31	$1/6\ A\ell^2$	2×10^8

Table 2. Non-zero Elements of the Upper Triangle of the Sampled Coupled System Unrestrained Stiffness Matrix, Contd.

ROW	COLUMN	ALGEBRAIC VALUE	NUMERIC VALUE
31	31	$2/3\ A\ell^2$	8×10^8
31	32	$1/6\ A\ell^2$	2×10^8
32	32	$2/3\ A\ell^2$	8×10^8
33	33	$1/3\ A\ell^2$	4×10^8
33	34	$1/6\ A\ell^2$	2×10^8
34	34	$2/3\ A\ell^2$	8×10^8
34	35	$1/6\ A\ell^2$	2×10^8
35	35	$2/3\ A\ell^2$	8×10^8
35	36	$1/6\ A\ell^2$	2×10^8
36	36	$1/3\ A\ell^2$	4×10^8
37	37	B + E	7.80711×10^8
38	38	B + E	7.80711×10^8
39	39	B + E	7.80711×10^8
40	40	B + E	7.80711×10^8
41	41	$1/3\ BS^2$	2.133×10^6
42	42	$1/3\ BS^2$	2.133×10^6
43	43	$1/3\ BS^2$	2.133×10^6
44	44	$1/3\ BS^2$	2.133×10^6
1	25	$-1/2\ A\ell$	-6×10^7
1	26	$-1/2\ A\ell$	-6×10^7
2	25	$1/2\ A\ell$	6×10^7
2	27	$-1/2\ A\ell$	-6×10^7
3	26	$1/2\ A\ell$	6×10^7
3	28	$-1/2\ A\ell$	-6×10^7
4	27	$1/2\ A\ell$	6×10^7
4	28	$1/2\ A\ell$	6×10^7
5	29	$-1/2\ A\ell$	-6×10^7

Table 2. Non-zero Elements of the Upper Triangle of the Sampled Coupled System Unrestrained Stiffness Matrix, Contd.

ROW	COLUMN	ALGEBRAIC VALUE	NUMERIC VALUE
5	30	$-1/2\ A\ell$	-6×10^7
6	29	$1/2\ A\ell$	6×10^7
6	31	$-1/2\ A\ell$	-6×10^7
7	30	$1/2\ A\ell$	6×10^7
7	32	$-1/2\ A\ell$	-6×10^7
8	31	$1/2\ A\ell$	6×10^7
9	33	$-1/2\ A\ell$	-6×10^7
9	34	$-1/2\ A\ell$	-6×10^7
10	33	$1/2\ A\ell$	6×10^7
10	35	$-1/2\ A\ell$	-6×10^7
11	34	$1/2\ A\ell$	6×10^7
11	36	$-1/2\ A\ell$	-6×10^7
12	35	$1/2\ A\ell$	6×10^7
12	36	$1/2\ A\ell$	6×10^7
13	17	-D	-10^8
16	20	-D	-10^8
17	21	-D	-10^8
20	24	-D	-10^8
1	37	-E	-7.8×10^8
4	38	-E	-7.8×10^8
9	39	-E	-7.8×10^8
12	40	-E	-7.8×10^8
5	37	-B	-0.711×10^6
5	39	-B	-0.711×10^6
8	38	-B	-0.711×10^6
8	40	-B	-0.711×10^6
5	41	-1/2 BS	-1.0665×10^6

Table 2. Non-zero Elements of the Upper Triangle of the Sampled Coupled System Unrestrained Stiffness Matrix, Contd.

ROW	COLUMN	ALGEBRAIC VALUE	NUMERIC VALUE
5	43	1/2 BS	1.0665×10^6
8	42	-1/2 BS	-1.0665×10^6
8	44	1/2 BS	1.0665×10^6
17	37	1/2 BS	1.0665×10^6
17	39	-1/2 BS	-1.0665×10^6
20	38	1/2 BS	1.0665×10^6
20	40	-1/2 BS	-1.0665×10^6
17	41	$1/6\ BS^2$	1.0665×10^6
17	43	$1/6\ BS^2$	1.0665×10^6
20	42	$1/6\ BS^2$	1.0665×10^6
20	44	$1/6\ BS^2$	1.0665×10^6
37	41	1/2 BS	1.0665×10^6
38	42	1/2 BS	1.0665×10^6
39	43	-1/2 BS	-1.0665×10^6
40	44	-1/2 BS	-1.0665×10^6
8	45	-A	-12×10^6
8	47	$-1/2\ A\ell$	-6×10^7
20	46	-C	-10^8
32	45	$1/2\ A\ell$	6×10^7
32	47	$1/6\ A\ell^2$	2×10^8
45	45	A	12×10^6
45	47	$1/2\ A\ell$	6×10^7
46	46	C	5.92×10^7
47	47	$1/3\ A\ell^2$	4×10^8

The non-zero elements of the matrix are listed in Table 2. For simplicity, the following substitutions are made:

$$\frac{12\ EI_{yy}}{\ell^3} = A \qquad = 12 \times 10^6$$

$$\frac{12\ EI_{xx}}{S^3} = B \qquad = 0.711 \times 10^6$$

vertical beam torsion spring rate = C = 5.92×10^7 n/m

lateral torsion spring rate = D = 10^8 n-m/rad

ball joint translational spring rate = E = 7.8×10^8 n/m

Eigenvalues and eigenvectors are found by operation on the reduced stiffness matrix and the associated diagonal mass-inertia matrix.

The only quantities remaining to be determined for use in the mode synthesis equations are the elastic component modes. These data were obtained readily, as the component systems are elementary, and are given below.

a. Elastic bending modes of outer tanks:

Mode	1	2
ω^2	416.18	2543.4
m	12975	21144
X_1	1	0.6667
X_2	-0.5	-1.0
X_3	-0.5	1.0
X_4	1	-0.6667

b. Elastic torsion modes of outer tanks:

Mode	1	2	3
ω^2	3700	11100	14800
m	24000	24000	48000
θ_1	1.0	1.0	1.0

θ_2	0.5	-0.5	-1.0
θ_3	-0.5	-0.5	1.0
θ_4	-1.0	1.0	-1.0

c. Elastic bending modes of center tank:

Mode	1	2	3	4
ω^2	5.299	195.42	1615.4	5706.7
$\mathfrak{M}$	9035.1	12064	18518	6237
X_1	1.0	1.0	0.81183	-0.11309
X_2	0.65377	-0.30099	-0.98959	0.22209
X_3	0.33546	-0.84158	0.57622	-0.40665
X_4	0.09552	-0.43767	1.0	1.0

d. Elastic torsion modes of center tank:

Mode	1	2	3	4
ω^2	583.73	5524.3	12976	17916
$\mathfrak{M}$	30399	25048	19791	11611
θ_1	1.0	1.0	1.0	-0.13856
θ_2	0.92112	0.25347	-0.75347	0.19692
θ_3	0.69692	-0.87151	0.13544	-0.42112
θ_4	0.36277	-0.69527	0.54938	1.0

The introduction of these data into the [TS] matrix developed above permits the solution of Equation 29 for eigenvalues and eigenvectors.

A comparison of the results of both techniques shows near perfect agreement. The discrepancy in the lowest frequency is but 0.49 percent and in the second frequency, 0.056 percent. The remaining frequencies show even better agreement. Theoretically, the two solutions should be equivalent; close examination of the data indicates the existing error results from numerical accuracy limitations of the

digital computer used, generated by the choice of a comparatively high value for the ball joint lateral stiffness. A stiffness of a magnitude more like the other stiffnesses of the system would have resulted in a problem with less numerical disparity and, consequently, greater agreement in frequency.

For comparative purposes, the frequencies and mode shapes for the first five modes are given in the following list for each technique.

STIFFNESS APPROACH

MODE	1	2	3	4	5
FREQUENCY CPS	1.9735007 -02	5.3441634 -01	7.4287665 -01	9.0677050 -01	1.1680276 +00
MODE SHAPE					
X_1	9.9999993 -01	-9.4764832 -01	-3.9673698 -01	9.6906630 -01	-7.0145900 -01
X_2	7.1568394 -01	-9.9999995 -01	1.2257424 -01	3.1318669 -01	-4.1447943 -01
X_3	4.2472581 -01	-9.7198812 -01	5.9307930 -01	-3.5356943 -01	-2.6789271 -02
X_4	1.2777052 -01	-8.6406809 -01	9.9999995 -01	-9.9999990 -01	4.3150822 -01
X_5	9.1627709 -01	-1.0882327 -08	-4.8267826 -01	5.1630496 -08	9.6583841 -01
X_6	5.8795033 -01	-4.8570223 -09	-2.7574998 -01	5.1650791 -08	1.0000000 +00
X_7	2.9631802 -01	-2.6235039 -09	-9.2177604 -02	3.7335925 -08	7.4372248 -01
X_8	8.3944520 -01	-1.1955026 -09	7.1434131 -03	1.3869443 -08	2.7490693 -01
X_9	1.0000000 +00	9.4764837 -01	-3.9673705 -01	-9.6906632 -01	-7.0145886 -01
X_{10}	7.1568397 -01	1.0000000 +00	1.2257420 -01	-3.1318674 -01	-4.1447942 -01
X_{11}	4.2472584 -01	9.7198812 -01	5.9307926 -01	3.5356943 -01	-2.6789353 -02
X_{12}	1.2777052 -01	8.6406809 -01	1.0000000 +00	1.0000000 +00	4.3150805 -01

STIFFNESS APPROACH, Contd.

MODE	1	2	3	4	5
FREQUENCY CPS	1.9735007 -02	5.3441634 -01	7.4287665 -01	9.0677050 -01	1.1680276 +00
MODE SHAPE					
θ_1	5.7221371 -11	4.5465852 -02	-2.8953498 -09	-1.7093574 -02	1.0148364 -08
θ_2	5.3688464 -11	4.1159983 -02	-2.6372581 -09	-1.2208383 -02	8.8684943 -09
θ_3	4.5610161 -11	3.6728686 -02	-2.3669080 -09	-7.2160877 -03	7.9541399 -09
θ_4	3.9882893 -11	3.2185467 -02	-2.0790094 -09	-2.1604849 -03	6.4575052 -09
θ_5	6.2903006 -11	4.7973918 -02	-3.0425455 -09	-1.9941218 -02	1.0747555 -08
θ_6	5.5707523 -11	4.1926386 -02	-2.5863277 -09	-1.3109496 -02	8.8646642 -09
θ_7	4.4919723 -11	3.5751090 -02	-2.1221440 -09	-6.1627592 -03	7.1508037 -09
θ_8	3.4295750 -11	2.9466850 -02	-1.9053834 -09	8.3804232 -04	4.7042680 -09
θ_9	6.0460436 -11	4.5465852 -02	-2.8947245 -09	-1.7093574 -02	1.0348846 -08
θ_{10}	5.2621624 -11	4.1159983 -02	-2.6376531 -09	-1.2208383 -02	9.2657280 -09
θ_{11}	4.6676823 -11	3.6728686 -02	-2.3636810 -09	-7.2160877 -03	7.6464065 -09
θ_{12}	3.6643896 -11	3.2185467 -02	-2.0774737 -09	-2.1604849 -03	6.3009331 -09

MODE SYNTHESIS

MODE	1	2	3	4	5
FREQUENCY, CPS	1.9638325 -02	5.3471664 -01	7.4330859 -01	9.0747551 -01	1.1684696 +00
MODE SHAPE					
X_1	9.9999991 -01	9.4763948 -01	-3.9619328 -01	-9.6898205 -01	-7.0205242 -01
X_2	7.1545291 -01	1.0000000 +00	1.2306283 -01	-3.1311603 -01	-4.1483323 -01
X_3	4.2433175 -01	9.7190802 -01	5.9338963 -01	3.5362816 -01	-2.6749588 -07
X_4	1.2727547 -01	8.6382077 -01	9.9999727 -01	1.0000000 +00	4.3204152 -01
X_5	9.1725025 -01	1.7466167 -07	-4.8283761 -01	-2.8418209 -07	9.6514644 -01
X_6	5.8849936 -01	1.1663936 -07	-2.7578723 -01	-1.8404749 -07	1.0000000 +00
X_7	2.9654573 -01	6.6066904 -08	-9.2116577 -02	-8.9023212 -08	7.4404868 -01
X_8	8.3991410 -02	2.4224830 -08	7.2151979 -03	-2.0534622 -08	2.7511672 -01
X_9	1.0000000 +00	-9.4763898 -01	-3.9619581 -01	9.6898152 -01	-7.0205230 -01
X_{10}	7.1545297 -01	-9.9999952 -01	1.2306206 -01	3.1311581 -01	-4.1483320 -01
X_{11}	4.2433179 -01	-9.7190754 -01	5.9339067 -01	-3.5362811 -01	-2.6749588 -02
X_{12}	1.2727549 -01	-8.6382032 -01	1.0000000 +00	-9.9999974 -01	4.3204134 -01
θ_1	4.8394264 -10	-4.5596325 -02	-2.1323593 -08	1.7139997 -02	-5.3995718 -10
θ_2	4.4602392 -10	-4.1277190 -02	-1.5027954 -08	1.2244480 -02	-7.1133706 -10
θ_3	4.0835142 -10	-3.6832129 -02	-8.6108861 -09	7.2413734 -03	-8.6280056 -10
θ_4	3.6966862 -10	-3.2274702 -02	-2.0998440 -09	2.1746317 -03	-9.3464032 -10

MODE SYNTHESIS, Contd.

MODE	1	2	3	4	5
FREQUENCY CPS	1.9638325 -02	5.3471664 -01	7.4330859 -01	9.0747551 -01	1.1684696 +00
MODE SHAPE					
θ_5	3.1749107 -10	-4.8112078 -02	-2.5013947 -08	1.9993565 -02	-2.2364372 -10
θ_6	2.6403497 -10	-4.2045909 -02	-1.6204447 -08	1.3147358 -02	-5.4393848 -10
θ_7	1.5573409 -10	-3.5851060 -02	-7.3368291 -09	6.1857681 -03	-7.6038114 -10
θ_8	1.4136948 -10	-2.9547560 -02	1.7858855 -09	-8.3052308 -04	-8.9794444 -10
θ_9	3.6576448 -10	-4.5596326 -02	-2.1057110 -08	1.7139997 -02	-4.5998652 -10
θ_{10}	3.3204248 -10	-4.1277190 -02	-1.4760028 -08	1.2244480 -02	-6.8724365 -10
θ_{11}	2.8444532 -10	-3.6832129 -02	-8.3151636 -09	7.2413734 -03	-9.1439566 -10
θ_{12}	2.5005513 -10	-3.2274702 -02	-1.8059722 -09	2.1746392 -03	-1.0430573 -09

5/REFERENCES

1. Nestorides, E. J., "A Handbook on Torsional Vibration," Cambridge University Press, 1958.

2. Myklestak, N. O., "Fundamentals of Vibration Analysis," McGraw-Hill Book Company, New York, N.Y., 1956, pg. 237-239.

3. Kiefling, Larry, "Multiple Beam Vibration Analysis of Saturn I and IB Vehicles," NASA TM X-53072, June 1964.

4. Milner, James L., "Three Dimensional Multiple Beam Analysis of a Saturn I Vehicle," NASA TM X-53098, July 1964.

5. Bodley, Ikard, and Schultz, "Vibration Analysis Report, Program 624A, Configuration C, Flight Plan VIII," SSD Report No. SSD-CR-65-1, January 1965.

6. Jacobsen, Lydik S., and Ayre, Robert S., "Engineering Vibrations," McGraw-Hill Book Company, New York, 1958, pg. 391-399.

7. Gravitz, Stanley I., "An Analytical Procedure for Orthogonalization of Experimentally Measured Modes," Journal of Aerospace Sciences, November 1958, pg. 721-722.

8. Storey, Richard E., "Dynamic Analysis of Clustered Boosters with Application to Titan III," AIAA 1963 Summer Meeting, Paper No. 63-208, June 1963.

9. Lianis, George, "Matrix Analysis of Vibrations of Clustered Boosters," GD/A Report AE61-0858, September 1961.

10. Timoshenko, S. and MacCullough, G. L., "Elements of Strength of Materials," D. Van Nostrand Company, Princeton, N. J., 1949, pg. 330-335.

11. Bodewig, E., "Matrix Calculus," North Holland Publishing Company, Amsterdam, 1959.

12. Faddeeva, V. N., "Computational Methods of Linear Algebra," Dover Publications, N. Y., 1959.

13. Bisplinghoff, R. A., Ashley, H., and Holfmann, R. L., "Aeroelasticity," Addison-Wesley Publishing Company, Reading, Mass., 1955.

14. Stodola, A., "Steam and Gas Turbines," translated by L. C. Loewenstein, vols. 1 and 2, McGraw-Hill Book Company, Inc., New York, 1927.

15. Holzer, H., "Die Berechung der Drehschwingungen," Springer-Verlay, Berlin, 1921.

16. Myklestad, N. O., "Vibration Analysis," McGraw-Hill Book Company, Inc., New York, 1944.

17. Lord Rayleigh, "Theory of Sound" (Vol. I, paragraphs 142 and 187), 1877.

18. Gieseke, R. K., Appleby, B. A., and Tonelli, W., "General Missile Vibration Program," GD/A Report GD|A-DDE64-050, August 1964.

NASA-Langley, 1967 — 32 CR-937